Dipl.-Ing. Peter Feenstra

Simulation of Solute-Solid Interactions

DISSERTATION

zur Erlangung des akademischen Grades

Doktor der technischen Wissenschaften

eingereicht an der

Technischen Universität Graz

Betreuer

Univ.-Prof. Dipl.-Ing. Dr. techn. Johannes Khinast

Institut für Prozess-und Partikeltechnik

Co-Betreuerin

Ass.-Prof. Dipl.-Ing. Dr.techn. Heidrun Gruber-Wölfler

Institut für Prozess-und Partikeltechnik

Graz, Dezember 2014

EIDESSTATTLICHE ERKLÄRUNG

Ich erkläre an Eides statt, dass ich die vorliegende Arbeit selbstständig verfasst, andere als die angegebenen Quellen/Hilfsmittel nicht benutzt, und die den benutzten Quellen wörtlich und inhaltlich entnommenen Stellen als solche kenntlich gemacht habe. Das in TUGRAZonline hochgeladene Textdokument ist mit der vorliegenden Dissertation identisch.

_____   _____

Datum   Unterschrift

Acknowledgement

Foremost, I would like to thank Johannes Khinast for the opportunity to work at the IPPE and write my doctoral thesis and for his scientific support and input.

I would also like to express my gratitude for Mic Brunsteiner's valuable advise and support during all stages of this work.

Further thanks go to Heidi Gruber-Wölfler who already supervised my diploma thesis and was always very helpful during my time at the IPPE.

Moreover, my gratitude goes to my colleagues at the IPPE. Thank you all for the very good times!

Very special thanks go to Verena and my family for the support during my time as PhD student.

Abstract

The aim of this thesis is to use computational simulation methods, in particular Molecular Dynamics to investigate solute-solid interaction phenomena in two different scientific fields. h

The first goal was to investigate issues encountered in pharmaceutical sciences. When pharmaceutical products come into contact with packaging material, interactions between the drug product and the packaging can have serious effects on the health and safety of patients. The experimental investigation of a great variety of different packaging material – drug product combinations in terms of efficacy and safety can be a costly and time-consuming task. In our work we used molecular dynamics (MD) simulations in order to evaluate the applicability of such methods to pre-screening of the packaging material-solute compatibility.

Diverse solute/solvent/solid systems were investigated and the results show that the use of a model for the interaction between the migrant and the polymer at atomistic detail can yield significantly better results when predicting the polymer solvent partitioning than simple empiric models based on the octanol water partition coefficient.

The second goal was to find a predictive tool in the area of separation sciences for the retention behavior of solutes in novel chromatographic systems.

Here, the investigation of the applicability of octanol water partition coefficient based retention time predictions for the separation in capillary electro-chromatography (CEC) is presented. The results indicate that rigorous simulation models are capable of accurately reproducing experimental results and that the electrophoretic mobility of analytes in CEC separations leads to significant deviations in the retention time prediction.

Table of Contents

Introduction

A Brief Historical Overview of the Science of Intermolecular Forces[1]

The intellectual pursuit to elucidate the interaction between substances is a core issue in science and philosophy throughout history. In ancient Greece the idea of indivisible particles ("atomos") was introduced by Demokrit and a first concept of attractive and repulsive forces was conceived by Empedokles who spoke of "love" and "hate" between elements. From these conceptual basics on many great and famous contributions to science led the way towards the modern understanding of intermolecular forces.

An early modern milestone is the gas law by Robert Boyle from 1662 stating that $pV = constant$ implies that gas molecules repel each other leading to increased pressure p when the Volume V containing the gas is decreased. 25 years later Isaac Newton formulated the law of gravity. Gravity suggests that gas molecules attract each other and this view is supported by the observation that they can condense into liquid and solids. So the forces acting on molecules had to be either repulsive or attractive depending on their distance. At long ranges they had to be attractive (gravitation) becoming repulsive (Boyle's law) at smaller distances then attractive accounting for condensation and ultimately becoming repulsive again since condensed matter cannot be compressed indefinitely.

After two centuries of controversy Johannes van der Waals published his equation of state for real gases in 1873. Based on the ideal gas law $pV = nRT$, an enhancement of Boyle's law by the observation that the pressure p is proportional to the temperature T at constant volume V for a number of molecules n with R being the gas constant, the van der Waals equation takes the finite size of molecules (*b*) as well as attractive forces between them (a/V^2) into account: $(p + a/V^2)(V - b) = nRT$. The attractive molecular forces are now known as van der Waals forces.

---

[1] This sub-chapter is based on the book "Intermolecular and Surface Forces, Third Edition" by Jacob Israelachvili, published by Academic Press, 2011

In 1903 Gustav Mie introduced the interaction pair potential $w(r) = -A/r^n + B/r^m$ that accounts for attractive as well as for repulsive interactions depending on the distance r with A, B, m and n being empirical constants. Still, the nature and origin of the intermolecular forces was not further elucidated until the 20th century. When quantum mechanics were developed and the electronic structure of atoms and molecules was recognized the intermolecular forces could finally be identified to stem from the electrostatic force one of the four fundamental forces in nature. So after solving the Schrödinger equation to determine the structure of the electron clouds of a system any intermolecular forces could be calculated using classical electrostatics. The major difficulty arises from the high difficulty to solve the Schrödinger equation for large systems. An exact solution can only be obtained for a single hydrogen atom in vacuum. For practical reasons there still exists a distinction between different intermolecular forces such as chemical bonds, van der Waals forces, hydrophobic interaction, hydrogen bonds or solvation forces though they stem from the same origin. Though often useful, such distinctions have to be handled with care because distinct interactions could be strongly coupled to each other. Recent research areas in the field of surface forces include for example colloidal systems, liquid structure, surface phenomena, complex fluids, soft matter as well as non-equilibrium systems. The increasing complexity of these topics often demands the introduction of computational methods.

A common problem when dealing with multicomponent systems at a molecular level is that the suspending medium cannot be regarded as a structureless continuum and a vast number of interactions between different molecules has to be regarded simultaneously. A computer can be used to calculate the interactions between a large number of molecules and predict their behavior according to an interaction potential (e.g. the Lennard-Jones potential, a special case of the Mie potential).

One of the most popular computational methods is Molecular Dynamics (MD) which is the method used in this thesis and is explained in more detail in one of the following chapters.

A Brief Glimpse at the Role of Computer Simulations[2]

Over the past 60 years molecular simulations have become a valuable tool in theoretical and applied sciences. Their rise in importance and applicability is coupled to the rise in computational power provided by modern electronics. Molecular simulations can serve as a first principle test for theoretical endeavors as well as computer experiments in support of experimental studies.

To better understand the role of computer simulations and how they work we have to look at some fundamental principles. In nature, all observed systems will, given enough time, reach a steady state where all macroscopic properties no longer change over time. Before a system reaches this steady state, the equilibrium, it is in the process of equilibration. A vast number of systems encountered across any scientific field is either in equilibrium or in the process of equilibration. The Second Law of Thermodynamics can be used to explain the driving source behind this equilibration process. In short, the system's entropy maximizes during the equilibration process until all its properties, like, e.g., pressure, temperature or concentration remain invariable over time. This concept provides us with the possibility to define the state of equilibrium for a given system. For example, in a system, though composed of a vast number of microscopic particles (molecules) only two of the experimentally accessible properties volume, temperature and pressure have to be known to specify the state of equilibrium.

Although this thermodynamic concept is of great importance and due to its applicability ubiquitously used in science it has a shortcoming, namely the inability to provide details about the microscopic mechanisms that lead to the macroscopic properties of a system. For example, the phenomenon of solubility or phase transition cannot be derived from thermodynamic principles but an explanation has to be found on the molecular or atomic level. Therefore, thermodynamics is not

---

[2] This subchapter is based on the journal article "Using Molecular Simulations to Probe Pharmaceutical Materials" by Yong Cui published in the Journal of Pharmaceutical Sciences, Vol. 100, No.6, 2011

suited for many mechanistic and predictive tasks. The search for an understanding of the relationship between microscopic particle properties and macroscopic observable system properties lead to the emergence of a statistical-mechanical perspective. With the introduction of statistical mechanics microscopic properties like particle velocities and positions can be related to macroscopic system properties. In a system with a large number of particles and consequently a large number of microscopic variables it becomes essential to view the system from a statistical perspective. It can then be postulated that all macroscopic system properties are either sums or averages of the underlying microscopic properties. For example, the temperature is the statistical average of the kinetic energy of the individual particles while the internal energy is the statistical sum of the energy of all particles. Central to the concept of statistical mechanics is the Boltzmann Distribution Law, which states that individual energy states of the particles in a system in equilibrium follow a particular distribution. Now although the microscopic properties like position, momentum or energy of each individual particle vary with time, the statistical sums and averages over all particles do not. When a system is not yet in equilibrium and the distribution of energy states does not follow the Boltzmann Distribution Law, the Boltzmann Distribution Law specifies the direction in which the system will evolve much like the Second Law of Thermodynamics does. Still, the question remains why particles tend to move towards lower energy states in equilibrium. The individual particle does not have a preference for a specific energy state. The reason why particles prefer lower energy states is that the macroscopic properties (e.g. the total energy) of a system at equilibrium can be achieved via any possible composition of microscopic properties to form a microstate and each microstate is equally probable to occur. So if, hypothetically, one individual particle combined the total energy of the system on itself there is only one microstate possible for the particle in which the system could exist. If the particle is in a lower energy state and other particles contribute to the total energy, it can be in a higher number of possible microstates while the criteria of the total energy of the system is still fulfilled. Therefore, the lower the energy of the individual particle is, the higher the number of probable microstates it can exist in is. The total number of possible microstates of a system is usually denoted with Ω and Boltzmann explained the concept of entropy that was introduced

by the Second Law of Thermodynamics without a clear physical meaning via the famous expression $S = k \ln\Omega$.

Statistical mechanics offer a mechanistic explanation for thermodynamics and other physical phenomena. However, it is extremely challenging to experimentally access microscopic particle states. In contrast, computer simulations are perfectly suited to evaluate microscopic particle states and can contribute tremendous assistance in the task of predictive modeling of macroscopic material properties from microscopic particle properties. More details on specific computational methods can be found in the following chapter.

Computational Methods used in this Thesis[3]

Molecular Dynamics (MD) is used to compute the equilibrium and transport properties of classical many-body systems. Classical means, that the motions of the regarded particles (atoms) are calculated using the laws of classical mechanics.

Each atom or a group of atoms is represented by a sphere with a given diameter and mass. The bonded interactions between the atoms are described by the mathematical model of a mechanical spring. The spring strength represents the molecular bond strength. The so called nonbonded interactions arise between atoms belonging to different molecules or atoms of the same molecule that are further apart. The nonbonded interactions are considered via a potential function dependent on the distance between the atoms (e.g. Lennard-Jones potential). When all of the interatomic forces are combined they form a so called force field. By knowing the force acting on each atom in the system Newton's equations of motion can be solved. This can only be done numerically in small timesteps. The typical timestep for MD simulations lies in the range of 1 fs. After each step the calculated coordinates and velocities form the input for the next step. This provides new atom positions, velocities and forces and the procedure can be repeated for the desired amount of time steps. Finally, one can follow the displacement of selected molecules and extract desired information.

Generally, The setup of a MD simulation follows similar rules as does a real experiment. The first step is to set up a system of a defined number of particles (sample preparation). Then the Newton's equations of motion are solved until the system is in equilibrium, e.g., its properties do no longer change over time. Then the actual measurement is performed. As is the case with most real measurements, a higher number of samples, i.e. the averaging over a longer simulation run reduces the statistical noise and yields a more accurate result. From the measured microscopic properties like particle momentum and position macroscopic properties

---

[3] This sub-chapter is based on the book "Understanding Molecular Simulations" by Daan Frenkel and Berend Smit, published by Academic Press, 2002

can be recalculated as sums or averages of thereof as described in the previous chapter. However, a very important property, namely the entropy and consequently the free energy cannot be calculated directly from the average particle momentum and position. For this task separate techniques like umbrella sampling to calculate the potential of mean force are used.

If we, for example, want to investigate the likelihood of one molecule to adsorb on a surface (difference in free energy between a "free" state and an adsorbed state) we can calculate the potential of mean force. The potential of mean force is the potential that gives the average force acting on a molecule when keeping the molecule artificially fixed. When we calculate the forces along a reaction coordinate, which in this case is the distance between the molecule and the surface, we get to know the change in the free energy of the system as a function of the reaction coordinate. So this way we can determine the free energy of adsorption of the API on the corresponding surface.

Now to get reasonable results for the PMF we have to cover all the positions of the molecule along the reaction coordinate. To do so we perform a method called umbrella sampling. This method can be used to overcome energy barriers like the local minimum of the curve on the last slide. When the energy barrier is high enough, normally we would never or only very rarely encounter a molecule to overcome this energy barrier. By pulling the molecule along the reaction coordinate we can artificially overcome this energy barrier and record all conformations of the molecule. Then we take one configuration on this reaction coordinate and fix the API molecule in place and calculate the forces acting on the molecule restrained in this place. This is called a sampling window. When we do this for a large enough part of the reaction coordinate and combine the results of the sampling windows we get the PMF curve for the adsorption process.

Further details on this method and other methods like the Linear Interaction Energy can be found in the following chapters.

Scope of the thesis

The aim of this thesis was to use computational simulation methods, in particular Molecular Dynamics to investigate solute-solid interaction phenomena in two different scientific fields.

The first goal was to investigate issues encountered in pharmaceutical sciences. When pharmaceutical products come into contact with packaging material, interactions between the drug product and the packaging can have serious effects on the health and safety of patients.

The second goal was to find a predictive tool in the area of separation sciences for the retention behavior of solutes in novel chromatographic systems.

In the following section a brief overview of the two topics is given.

Drug-Packaging Interactions

To provide safe and effective therapeutic products to patients is an obligation in the area of medicine and pharmaceutical science. Only recently, the impact of the relation between drugs and materials they come in contact with during their lifetime is coming to notice. While for example plasticizers from packaging material that are found in food or beverages have made their way to public attention, drug product (DP) - container-material interactions remain an widely ignored issue in medicine. It must be remembered, though, that if they are pronounced, they can have a serious impact on the safety and efficacy of drugs that are administered to the patient.[1]

Those interactions can be divided into different phenomena. Smith [2] defines the four general types of DP - container-material interactions:

Adsorption occurs when a drug ingredient is concentrated at the surface of the container material.

Absorption occurs when a drug ingredient is dispersed into the container material matrix.

Permeation is the transmission of a drug ingredient through the container-material into the atmosphere or transmission of an outside material into the container.

Leaching is the process by which container-material ingredients migrate into the drug product.

The potential adverse effects of leaching processes mainly relate to the patients safety, either directly (e.g., via the toxicity of leached substances) or indirectly (e.g., by altering the drug product's properties, such as a pH change caused by alkali ions leaching from glass containers or chemical reactions with drug ingredients). Changes of stabilities cause a loss of content, loss of activity, reduce the duration of use, lead to the occurrence of side effects and adverse reactions. Sorption processes can also directly or indirectly affect the efficacy and stability of a drug product, e.g., via the loss of an important component, such as an active pharmaceutical ingredient (API), a stabilizer or other components critical to the stability or efficacy of a drug product.[1,3] Furthermore, there is the possibility that the process of leaching/sorption not only affects the drug but also the container material, causing swelling or brittleness that may result in the loss of its desired functions.[4]

During its lifetime a drug product repeatedly interacts with container-materials. These interactions can be either long-term, e.g., during storage in a shipping container, or short-term, e.g., during administration via an intravenous (IV) line).[5] The latter

includes, for example, parenteral drug administration, nutrition and dialysis.[6] For repeated applications, such as dialysis, the amount of leached toxic components is critical due to the patients' lifetime exposure. During parenteral drug administration, API may be dispersed or absorbed into a container-material, massively decreasing the dose that is administered to the patient and thus jeopardizing the success and effectiveness of the therapy.[7]

A prominent affair often cited in the context of DP – container-material interactions is the "Eprex" case. A change of components in the Eprex formulation, namely the replacement of human serum albumine by Sorbitol 80, led to the extraction of organic compounds from rubber closures. In succession micelles formed in the new Eprex formulation causing pure red cell aplasia in several patients.[8]

For other highly potential drugs that are for example used for cancer treatment, the knowledge of the administered dose is of particular importance. Since here, the therapeutic effect can only be monitored months after initial treatment an insufficient dose can have fatal consequences for the patient. On the contrary, a higher dose is in most cases accompanied by adverse effects, also threatening the patient's health.

Hospital pharmacy, for example, assumes exact dosing. The hospital pharmacy produces ready-to-use (RTU) infusions by partition of liquid concentrates. To receive correct final concentrations in the prepared infusion an exact volumetric sampling by using syringes is essential. Interactions between the drug and syringe can reduce the calculated dosage.

With regard to the patients' safety, a prediction of dose fluctuations would be particularly beneficiary. In this context the main parameters influencing dose fluctuations need to be examined and understood. State of the art prediction models are based on only a few parameters, namely the polarity of the drug solution, the lipophilicity of the migrating component described via its octanol/water partition coefficient ($P_{O/W}$) and an empirical constant for the container material.

However, in clinical environments, as in the case of IV drug administration these simple models fail due to the lack of a more rigorous consideration of relevant parameters. I.e., dynamic systems require the introduction of kinetic parameters that

are needed to display the dose to time relationship during the administration to the patient. Furthermore, the increasing complexity of drug products (e.g., emulsions with various additives, such as stabilizers, etc.) exacerbates the successful prediction of the behavior of single drug components in such a system. Especially the alteration of transport processes on a molecular level, e.g., by the presence of cosolvents or a surfactants, render the former mentioned polarity-based predictions useless and make the prediction of a dose time relation a complex optimization problem. Here, the implementation of computational methods could lead to significant improvement of the understanding of such systems.[9,10]

Chromatography

Liquid chromatography (LC) has evolved to become one of the most important techniques for the separation, isolation and purification of substances.[11]

It is widely used in the chemical and pharmaceutical industry and its applications are widespread, ranging from small scale analytical purposes with high sensitivity and resolution to large scale preparative purposes with a high throughput, e.g., for the purification of biotechnologically manufactured proteins.[12]

In general the different interactions of the solutes with the stationary phase can be attributed to polar and non-polar retention forces. Polar van der Waals forces arise from dipole interaction and hydrogen bonding. The resulting average association energy (ϵ_D) is mainly a function of the dipole moments of the involved components and the distance (Eq. 1).[11]

$$\in_D = -\left(\frac{2\,\mu_A{}^2\,\mu_S{}^2}{r^6\,kT}\right) \qquad\qquad \text{Eq. 1}$$

μ   dipole moment of the component A and S [A s]

r   distance between components [m]

k   Boltzmann constant [1.3806504*10-23 J/K]

T   Temperature [K]

The unpolar dispersion forces result from induced dipole interactions. These forces are called London forces ($\in_L$) and can be calculated according to Eq. 2.[11]

$$\in_L = -\left(\frac{3\,\alpha_A\,\alpha_S\,I_A\,I_S}{2r^6\,(I_A + I_S)}\right) \qquad\qquad \text{Eq. 2}$$

α   polarisability

I   ionisation potential

Since the separation in chromatography is mainly achieved via differences of the polarity of the stationary phase as well as of the solute molecules a short explanation on common techniques is given.

The surface of bare silica is covered with silanol-groups (Si-OH) which can be used for normal phase chromatography (NP). Characteristic for this kind of chromatography is that the mobile phases are less polar than the stationary phases. Therefore, this material is used for the separation of not very polar molecules that are hardly soluble in water and water mixtures.[13]

Functionalization of the silanol groups on the surface can yield a wide variety of different stationary phases. A very commonly used form is the so called reversed phase (RP).

In this case a stationary phase is used that is non-polar while the solvent is polar (often water mixed with a less polar component e.g. methanol). The non-polar stationary phases are usually obtained by the functionalisation of normal phases. Common functionalizations are octyl (C8) or octadecyl (C18) chains that lead to a hydrophobic surface where the analytes are retained in the order of their hydrophobicity. The hydrophobicity of the stationary phase can be influenced by the length and the amount of the alkyl chains.[14,15]

Due to the different forces between the different solute molecules and the stationary phase the solute molecules move with different velocities. The interaction or affinity to the stationary phase can be expressed via the ratio of concentrations of a component in each phase resulting in a distribution coefficient (Eq. 3).[11]

$$K_A = \frac{[A_S]}{[A_M]}$$
Eq. 3

K   distribution coefficient

A   component A

[A_S]   concentration of A in the stationary phase

[A_M]   concentration of A in the mobile phase

The larger the value of K the more the component is retained.

Figure 1 shows how a typical chromatogram emerges as the different concentrations are measured by a detector with respect to the elapsed time or mobile phase volume. The resulting chromatogram can then be interpreted leading to key parameters that form a valuable tool for the description of the performance of a chromatographic separation.

The time a solute needs through the chromatographic bed (retention time t_R) is the time a non-interacting solute (the mobile phase) would need (hold up time t_M) plus the time it spends in the stationary phase (adjusted retention time t'_R) (Eq. 4).

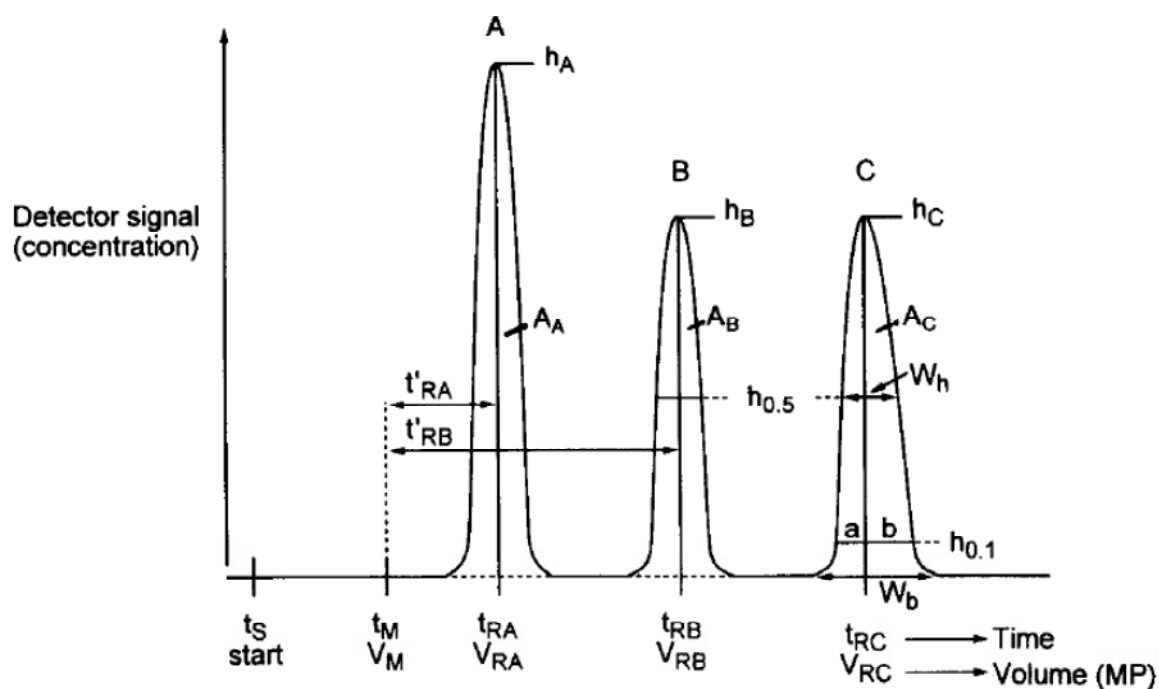$$t_R = t_M + t'_R$$ Eq. 4

Figure 1 Example of a chromatogram [11]

For the comparison of the separation performance the retention factor (k) is introduced. It takes the volumes of the phases (V_M, V_S) into account and therefore, resembles the ratio of solute molecules in each phase (Eg. 5).[11]

$$k = K \frac{V_S}{V_M}$$

Eq. 5

The retention factor can also be expressed using the adjusted retention time (Eq. 6).

$$k = \frac{t'_R}{t_M}$$

Eq. 6

By relating the k-values for two different components the ability of a stationary phase for the separation of these components can be displayed by the separation (or selectivity) factor α (Eq. 7):[11]

$$\alpha = \frac{k_B}{k_A}$$

Eq. 7

where k_B and k_A are the retention factors for the compounds A and B.

By definition the value for α has to be > 1, what means that the k-value for the more retained component is the numerator.

A very feasible approach to predict the retention behaviour of analytes in reversed phase chromatography would be an evaluation of their octanol-water partition coefficient $P_{o/w}$. The octanol-water partition coefficient (often used in the logarithmic form log $P_{o/w}$) is widely used in pharmaceutical science, for example to characterise the distribution of an analyte into biological membranes and can be directly related to the retention time t_c in a chromatographic separation (Eq. 8).[16]

$$\log P_{o/w} = \log t_c + const \tag{8}$$

with

$$t_c = \frac{(t_R - t_0)}{t_0} \tag{9}$$

t_R is the retention time of the analyte and t_0 is the retention time of a completely unretained component.

Alternatively, the log $P_{o/w}$ can also be calculated using the solvation free energy $\Delta_{solv}G$ of the analytes in two different solvents.

The solvation free energy in two solvents is related to the partition coefficient via Eq. 10:

$$P_{o/w} = \exp\left(\frac{\Delta_{hyd}G - \Delta_{oct}G}{RT}\right) \tag{10}$$

$P_{o/w}$ denotes the octanol water partition coefficient that is frequently used to describe the hydrophilic and hydrophobic properties of solute molecules. In this expression $\Delta_{hyd}G$ is the solvation free energy in water and $\Delta_{oct}G$ is the solvation free energy in octanol. R and T denote the gas constant and thermodynamic temperature, respectively.

A major benefit of such an approach for the prediction of chromatographic separation behaviour is the ability to easily adjust the solvent and even be able to use solvent mixtures.

The three following chapters are taken from published articles and deal with the simulation of various aspects of solute-solid interactions.

The chapter "Prediction of Drug-Packaging Interactions via Molecular Dynamics (MD) Simulations" deals with the influence of the liquid phase composition on the partitioning of an active pharmaceutical ingredient between a polymer solid phase and the liquid phase.

The chapter "Investigation of Migrant – Polymer Interaction in Pharmaceutical Packaging Material using the LIE Algorithm" investigates the free energy differences between a polymer solid phase and a liquid phase for a set of various small molecules. Each of the small molecules is of similar molecular weight but bears different chemical functionalities in order to elucidate the solute influence on the partitioning behavior.

The chapter "Retention-time Prediction for Polycyclic Aromatic Compounds in Reversed-phase Capillary Electro-chromatography" deals with the prediction of chromatographic retention times for different solutes and investigates the solid phase influence on the partitioning behavior.

References

[1]   D. Jenke, Compatibility of Pharmaceutical Products and Contact Materials, John Wiley & Sons, Inc., Hoboken, New Jersey, 2009.

[2]   E.J. Smith, in:, J. Swarbrick (Ed.), Encycl. Pharm. Technol., 3rd ed., Taylor & Francis Ltd, 2007, pp. 1466–1481.

[3]   R.G. Iacocca, M. Allgeier, J. Mater. Sci. 42 (2007) 801.

[4]   D. Jenke, J. Pharm. Sci. 96 (2007) 2566.

[5]   D.R. Jenke, J.M. Jene, M. Poss, J. Story, T. Tsilipetros, A. Odufu, W. Terbush, Int. J. Pharm. 297 (2005) 120.

[6]   S. Loff, F. Kabs, K. Witt, J. Sartoris, B. Mandl, K.H. Niessen, K.L. Waag, J. Ped. Surg. 35 (2000) 1775.

[7]   A. Treleano, G. Wolz, R. Brandsch, F. Welle, Int. J. Pharm. 369 (2009) 30.

[8]   C.L. Bennett, S. Luminari, A.R. Nissenson, M.S. Tallman, S. a Klinge, N. McWilliams, J.M. McKoy, B. Kim, E.A. Lyons, S.M. Trifilio, D.W. Raisch, A.M. Evens, T.M. Kuzel, G.T. Schumock, S.M. Belknap, F. Locatelli, J. Rossert, N. Casadevall, N Engl J Med 351 (2004) 1403.

[9]   D. Hofmann, L. Fritz, J. Ulbrich, C. Schepers, M. Böhning, Macromol. Theory Simul. 9 (2000) 293.

[10]   O.G. Piringer, A.L. Baner, Plastic Packaging, Wiley VCH Verlag GmbH & Co. KGaA, Weinheim, 2008.

[11]   A. Braithwaite, F.J. Smith, Chromatographic Methods, Kluver Academic Publishers, Dordrecht, 1999.

[12]   R.Q. Thompson, J. Chem. Educ. 77 (2000) 453.

[13]   R.J. Hurtubise, in:, J. Cazes (Ed.), Encycl. Chromatogr., Taylor and Francis Group, Boca Raton, 2005.

[14]   J.J. Pesek, M.T. Matyska, in:, J. Cazes (Ed.), Encycl. Chromatogr., Taylor and Francis Group, Boca Raton, 2005.

[15]   H. Minakuchi, K. Nakanishi, N. Soga, N. Ishizuka, N. Tanaka, Anal. Chem. 68 (1996) 3498.

[16]   M. Mirrlees, S. Moulton, C. Murphy, P. Taylor, J. Med. Chem. 19 (1976) 615.

Prediction of Drug-Packaging Interactions via Molecular Dynamics (MD) Simulations[4]
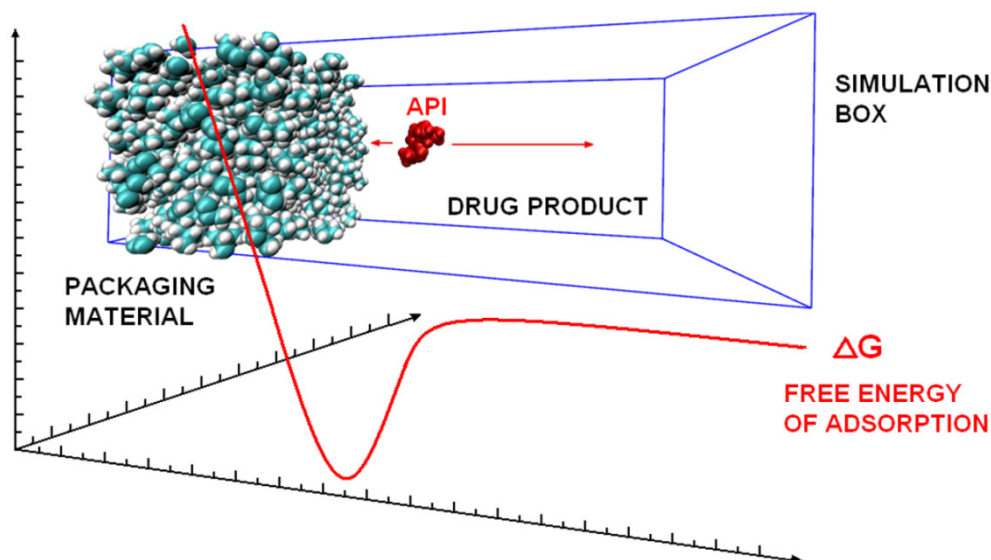
The interaction between packaging materials and drug products is an important issue for the pharmaceutical industry, since during manufacturing, processing and storage a drug product is continuously exposed to various packaging materials. The experimental investigation of a great variety of different packaging material – drug product combinations in terms of efficacy and safety can be a costly and time-consuming task. In our work we used molecular dynamics (MD) simulations in order to evaluate the applicability of such methods to pre-screening of the packaging material-solute compatibility. The solvation free energy and the free energy of adsorption of diverse solute/solvent/solid systems were estimated. The results of our simulations agree with experimental values previously published in the literature, which indicates that the methods in question can be used to semi-quantitatively reproduce the solid-liquid interactions of the investigated systems.

---

[4] This chapter is taken from a journal article by Feenstra et al. in the International Journal of Pharmaceutics (2012)

Introduction

Drug-packaging interactions can be an issue for the pharmaceutical industry since, if pronounced, they have an impact on the safety and efficacy of drug products.[1] The interactions between primary packaging materials and drug products, which result from mass transport of components (and possible reaction) between the packaging material and the drug, can be divided into two phenomena: leaching and sorption. Leaching occurs when chemical components migrate out of the packaging material into the drug product. Sorption is the inverse process, i.e., when the components initially present in the drug product move into the packaging material.[2] Sorption can subsequently be divided into (i) adsorption during which accumulation of the drug's component occurs at the surface of the packaging material, (ii) absorption during which dispersion of the drug's component in the packaging material is observed, and (iii) permeation during which a drug formulation's component passes through the primary packaging material into the surrounding secondary packaging or the environment.[3]

The potential adverse effects of leaching processes mainly relate to the product's safety, either directly (e.g., via the toxicity of leached substances) or indirectly (e.g., by altering the drug product's properties, such as a pH change caused by alkali ions leaching from glass). Sorption processes can directly or indirectly affect the efficacy and stability of a drug product, e.g., via the loss of an important component, such as an active pharmaceutical ingredient (API), a stabilizer or other components critical to the stability or efficacy of a drug product.[1,4]

Leaching and sorption processes are often associated with polymeric packaging materials (plastics) due to the widespread use of polymer components in drug manufacturing, processing and storage[5] and to their well-documented potential to release components that may cause adverse effects (e.g., plasticizers) [6]. The mobility of small molecules in polymers can be much higher than that in other packaging materials, e.g., glass, which gives rise to sorption processes.[7] Leaching and sorption are a potential threat to the integrity of a packaging material, causing swelling or brittleness that may result in the loss of its desired functions.[5]

During its lifetime a drug product repeatedly interacts with a packaging (or manufacturing) material. These interactions can be either long-term, e.g., during storage in a shipping container, or short-term, e.g., during administration via an intravenous (IV) line.[8] The latter includes, for example, parenteral drug administration, nutrition and dialysis.[6] For repeated applications, such as dialysis, the amount of leached toxic components is critical due to the patients' lifetime exposure. During parenteral drug administration, API may be dispersed or absorbed into a packaging material, massively decreasing the dose that is administered to the patient and thus jeopardizing the success and effectiveness of the therapy.[9]

Based on experimental data and heuristic assumptions, sorption and leaching can be mathematically modeled. The parameters that influence these processes include the physical and chemical natures of the drug product, the migrating component and the packaging material, as well as the migrating component's concentration, the environmental temperature and the contact time of the system.[10]

The increasing complexity of drug products (e.g., emulsions with various additives, such as stabilizers, etc.) exacerbates the analysis of the components' migration between a drug product and packaging material, rendering the successful design of drug formulations a complex optimization problem.[11]

With regard to the patients' safety, predicting the mass transport of a migrating species between two contacting phases is particularly important. In this context the main parameters that need to be examined and understood are the partition and diffusion coefficients.[12] Jenke et al.[13] showed that partitioning of a migrating component between a specific packaging material and a solution in equilibrium was linearly dependent on the component's octanol/water partition coefficient ($P_{o/w}$) and on the polarity of the solution.

However, for non-equilibrium conditions, such as IV drug administration, kinetic parameters of the mass transfer are also required. Furthermore, when migration mechanisms are altered, e.g., by the presence of a cosolvent or a surfactant, polarity-based predictions may not be sufficient and additional information on the mass transfer process may be needed.[14] Here, experimental approaches are

expensive and time consuming, and, especially, the detailed analysis of interfacial mass transport involving complex mixtures is a major challenge.

In contrast, computational models can be used to obtain more detailed and mechanistic insights into leaching and sorption processes.[12,15] Theoretically, it is possible to explicitly describe, for example, a polymer at the atomistic level exhibiting all microscopic and macroscopic properties of the true polymer.[15,16] Among the many computational methods, molecular dynamics (MD) simulations are widely used to study intermolecular interactions in the field of biochemistry and in material sciences.[17] In this work we used MD simulations to estimate two relevant material properties: (1) the solvation free energy $\Delta_{solv}G$ [18], and (2) the free energy of adsorption. In the case of the free energy of adsorption two different methodologies were used to evaluate the applicability of such calculations towards the investigation of leaching and sorption processes: 1) direct calculations of the potentials of mean force (PMF) between a molecule in solution and a container wall [19,20] and 2) the linear interaction energy algorithm (LIE).[21] The PMF was calculated using the technique of umbrella sampling, which is frequently applied to describe molecular interactions. The resulting PMF curves emerged as a function of the interspecies distance.[17]

Two migrating components were considered in our study, the first one being 2,6-diisopropylphenol, a small-molecule API consisting of a phenol unit substituted with two isopropyl groups in ortho position to the hydroxyl group (see Figure 1). The other migrating component was 3-(3,5-di-tert-butyl-4-hydroxyphenyl)propionic acid.
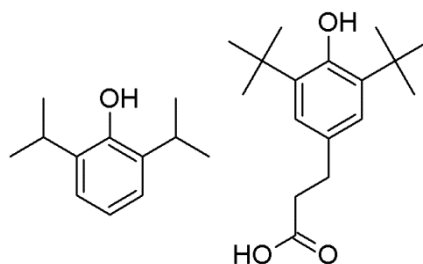

Figure 1. Chemical structures of the investigated compounds 2,6-diisopropylphenol (left) and 3-(3,5-di-tert-butyl-4-hydroxyphenyl)propionic acid (right)

Methods

2,6-diisopropylphenol was chosen as the migrating species primarily because of its clinical application as the API in anesthetic drugs, such as propofol and diprivan. It is administered via plastic syringes and IV lines [22] and may be expected to (strongly) interact with the hydrophobic environment of the polymeric packaging material due to its strong hydrophobicity (solubility in water: 150 mg/L).[23] The second substance 3-(3,5-di-tert-butyl-4-hydroxyphenyl)propionic acid is an antioxidant decomposition product encountered in polyethylene materials.[13] It was considered since it is initially present in the packaging material and, in contrast to 2,6-diisopropylphenol, migrates into the solution. Furthermore, experimental data for 3-(3,5-di-tert-butyl-4-hydroxyphenyl)propionic acid are available in the literature.

For our simulations all components were manually sketched using the AMBER11 [24–26] module xleap. The solvents used were water, ethanol, dimethylsulfoxide (DMSO), octane and octanol. The corresponding OPLS-AA (Optimized Potentials for Liquid Simulations – All Atoms) force field [27] parameters (including charge) were applied to all atoms and simple point charge (SPC) water was used.[28] All MD simulations were performed using the GROMACS software package version 4.5.3.[29–32]

For the calculation of the free energy of solvation the migrating component was put inside a cubic box with the side length of 3 nm followed by solvation with the appropriate solvent at ambient density. Periodic boundary conditions were applied and all distance-dependent properties were cut off at 1 nm. Long-range electrostatics was accounted for using particle mesh Ewald.[33] The box was equilibrated at the temperature of 300 K. The pressure of 1 bar was held constant by a Parrinello-Rahman barostat [34] with a time constant of 0.5 ps and compressibility of 4.5×10^{-6} bar^{-1}. 5,000 steps of steepest descent minimization were followed by 100,000 steps of equilibration. The equations of motion were solved using an sd integrator [35] with a time step of 2 fs. Production runs for the calculations of free energies of solvation were performed at the following λ-values: {0.0, 0.05, 0.10, 0.15, 0.20, 0.25, 0.30, 0.35, 0.40, 0.45, 0.50, 0.55, 0.60, 0.65, 0.70, 0.75, 0.80, 0.85, 0.90, 0.95, 1.00}. Here, λ denotes the coupling parameter describing interactions between the solute

and the solvent. At λ = 0 all interactions were switched on and at the value of λ = 1 all interactions were switched off. Each run included 5 ns simulation time. The ΔG_{solv} values were calculated using the GROMACS utility *g_bar*.[36,37]

The calculation of the LIE [38,39] is computationally less expensive than, for example, umbrella sampling because it requires only two MD simulations for each investigated system: one with the migrating component in solution and the other with the migrating component bound to the packaging material. For the LIE calculations a solute-solvent-solid simulation system was generated. The polymeric packaging material (polypropylene, cyclic olefin copolymer and polyethylene respectively) was introduced. Polypropylene (PP) and polyethylene (PE) are commonly used in packaging materials and are built from propene and ethene monomeric units, respectively, as depicted in Figure 2. Cyclic olefin copolymers (COC) belong to a relatively new class of polymeric packaging materials.[40] In our work COC made from norbornene and ethene (see Figure 2) with the molar ratio of the monomers of 6:5 was used. Starting coordinates were generated in such a way that the polymeric chains were aligned along the z-axis. Via this procedure, a PP chain with a molecular weight of 15 kDa, a COC chain of 35 kDa and a PE chain of 24 kDa were generated.
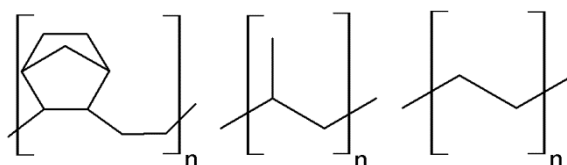

Figure 2. Structural motives of COC, PP and PE

To create a random packing of the polymer chain inside a simulation box, periodic boundary conditions were applied only in the x- and y-directions. In the z-direction walls were used to simulate a "die casting" process, where the system was compressed in the z-direction at the pressure of 1,000 bar and the temperature of 600 K using a Berendsen barostat [41] and a v-rescale thermostat.[42] After equilibration for 1 ns at the elevated pressure and temperature the system was brought to ambient conditions (300 K, 1 bar) and re-equilibrated for 1 ns. A final

conformation of the entangled polymer chain inside the cubic box with a side length of approximately 3 nm was produced. The final density reached was 855 kg/m³ for PP, 910 kg/m³ for PE and 960 kg/m³ for COC, which was close to the real values.[43,44] The migrating component was added to the system and randomly placed on the polymer surface. After 100 ps of equilibration the final coordinates were used as a start conformation for the solid-liquid interaction systems. The simulation setup is schematically displayed in Figure 3.
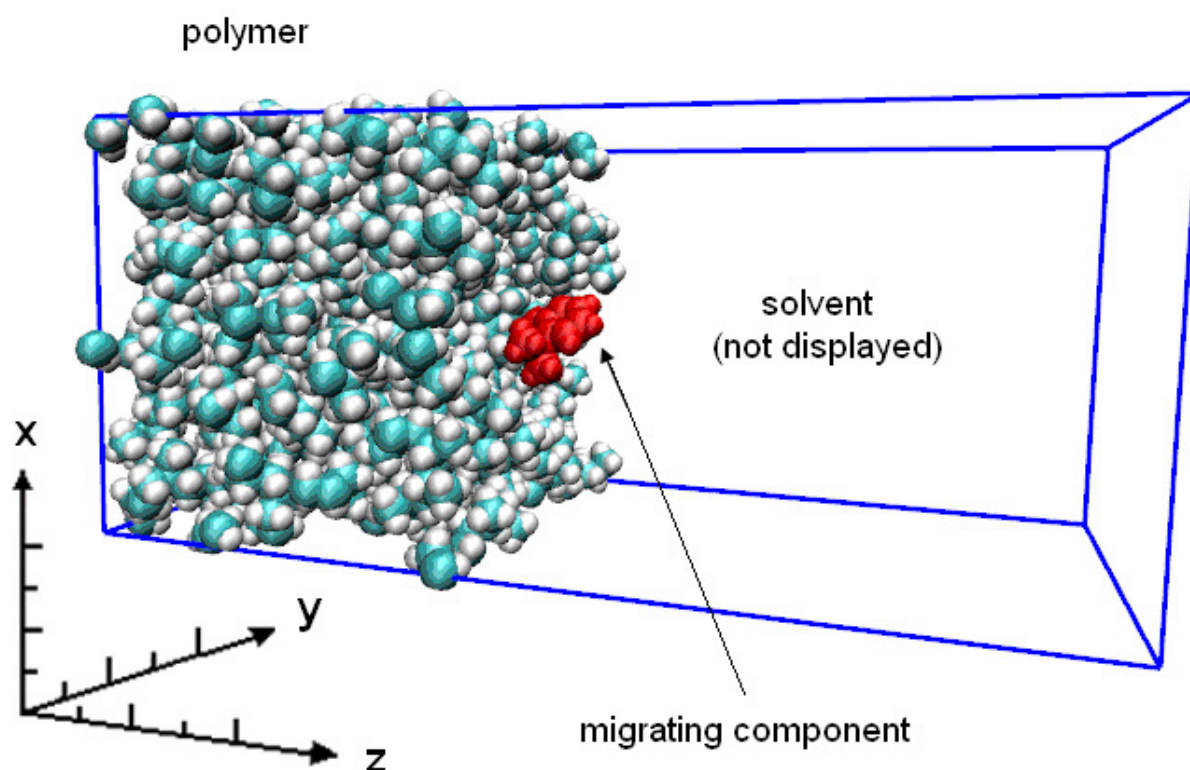

Figure 3. Simulation setup for the LIE calculations

First, the LIE between the migrating component and the packaging material was investigated. A respective solvent (water, ethanol, water/ethanol 50 v% and DMSO) was added to the start conformation to form a rectangular simulation system of 3 x 3 x 6 nm with periodic boundary conditions in all directions. After energy minimization and equilibration for 100 ps, a production run of 1 ns was performed. The electrostatic and van der Waals interactions in this bound state were calculated

using the GROMACS utility *g_lie* with default parameters. Interactions in a free state, i.e., the migrating component in the pure solvent, were obtained from the 1 ns production run in a 3 x 3 x 3 nm box similarly to the free enthalpy of solvation calculations.

The second method used to investigate the solid-liquid interaction was an explicit calculation of the free energy of adsorption as the potential of mean force obtained from umbrella sampling calculations. The starting conformation (polymer and migrating component) was generated as described above for the LIE calculations. The box for the umbrella sampling simulations was 3 x 3 x 7 nm. The respective solvent was added and the system was equilibrated for 100 ps. Because the calculation of ΔG_{solv} and LIE values with particle mesh Ewald (PME) electrostatics would be computationally very demanding, a reaction field was employed.[45] However, for umbrella sampling calculations PME is easy to implement and more accurate than a reaction field. Thus, PME was used for the umbrella sampling calculations. As proposed by Lemkul and Bevan [17] the Nosé-Hoover thermostat[46] was used along with the Parrinello-Rahman barostat.[34] To generate the starting configurations, the migrating component was pulled away from the surface for each solid-liquid combination, while the polymer was fixed with a position restraint on all heavy atoms of 1,000 kJ mol^{-1}. The pulling was performed by applying a harmonic potential between the centers of mass of the polymer and the migrating component. The force constant of the potential was set at 1,000 kJ mol^{-1} nm^{-2} and the reference position of the potential was changed at a rate of 0.01 nm ps^{-1} (pull rate). Each pulling simulation was conducted for 250 ps with a time step of 1 fs. Starting conformations for individual umbrella sampling windows were generated based on the resulting trajectory. The window's spacing was 0.05 nm within 0.5 nm from the surface and 0.1 nm beyond that distance (preliminary simulations showed that the PMF curve levels off towards a constant value within a distance of 1 nm from the surface). The force constant of the umbrella biasing potential was set to 10,000 kJ mol^{-1} nm^{-2} in direct vicinity to the surface and was linearly decreased to 1,000 kJ mol^{-1} nm^{-2} at a distance of 1 nm from the surface. Following this procedure, twenty sampling windows were generated for each solid-liquid combination, and the results were analyzed using the weighted histogram analysis method (WHAM).[47]

Results and Discussion

Free Enthalpy of Solvation

The solvation free energy in two solvents is related to the partition coefficient via Eq. (1):

$$P_{o/w} = \exp\left(\frac{\Delta_{hyd} G - \Delta_{oct} G}{RT} \right) \quad (1)$$

$P_{o/w}$ denotes the octanol water partition coefficient that is frequently used to describe the hydrophilic and hydrophobic properties of solute molecules. In this expression $\Delta_{hyd}G$ is the solvation free energy in water and $\Delta_{oct}G$ is the solvation free energy in octanol. R and T denote the gas constant and thermodynamic temperature, respectively.

Table 1 Calculated values for the solvation free energy of 2,6-diisopropylphenol in different solvents

Solvent	$\Delta_{solv}G$ (kJ mol^{-1})		
Water	-8.07	+/-	0.17
Octanol	-37.11	+/-	0.35

The calculated values displayed in Table 1 support the assumption that the solute molecule 2,6-diisopropylphenol is highly soluble in organic solvents and less soluble in water. Furthermore, according to the calculated values, a log $P_{o/w}$ for the solute molecule of 5.05 was obtained using Eq. (1). The experimental value for the log $P_{o/w}$ of 2,6-diisopropylphenol found in the literature is 4.16.[23] Though deviating from the experimental value, the difference between the calculated and the experimental value lies within an acceptable range. Nevertheless, the calculation of the log $P_{o/w}$ was mainly performed to check the general validity of the chosen OPLS-AA parameters for the following more elaborative simulation setup.

Linear Interaction Energy

The LIE was used to calculate the binding free energy of 2,6-diisopropylphenol to the surface of the packaging material in different solvents. The obtained values are displayed in Table 2. The investigated environments were created by placing the migrating component in close vicinity to the surface of the two polymers (PP and COC) representing the "bound state" in which the migrating component was bound to the surface and adding different solvents. The LIE values for the "free state," in which the migrating component was dissolved in a pure solvent, were calculated as well.

Table 2 Calculated values of the linear interaction energy for 2,6-diisopropylphenol in different environments

Solvent	LIE values (kJ mol^{-1})		
	PP	COC	Pure solvent
Water	-36.9	-32.0	-45.5
DMSO	-41.0	-40.1	-43.3
Ethanol	-34.3	-33.2	-35.4
Octane	-18.5	-18.1	-18.4

Interestingly, the difference in the LIE values for the bound state and the free state was only significant for the solvent "water" yielding the binding free energy ΔG_{bind} of +8.6 kJ mol^{-1} for PP and the value of +13.5 kJ mol^{-1} for COC. For all organic solvents there was no significant difference between the "bound state" and the "free state". A possible explanation for this lack of difference in binding free energies for the systems containing organic solvents could be that the LIE algorithm failed to fully account for entropic contributions. The fact that for the solvent "water" the binding free energy is even significantly positive implies that there is no tendency of the migrating component to bind to the polymer surface. This finding does not agree with a visual analysis of the simulated trajectory. In the case of water the migrating component never leaves the polymer surface during the simulation. Moreover, test simulations in which the migrating component was placed at 1 nm distance to the polymer surface showed a tendency of the migrating component to rapidly adsorb to

the surface. It is likely that, while the migrating component strongly interacts with water (an explicitly negative LIE value), it is the difference in the water-water interactions between the bound and the free state of the solvent not captured by LIE calculations, that accounts for this effect. This results in an overall poor solubility of the migrating component and the tendency to leave the hydrophilic aquatic environment and move towards the hydrophobic polymer surface.

Umbrella Sampling

The umbrella sampling simulations were used to investigate the difference in the free energy ΔG with respect to the distance of the migrating component to the polymer surface. The following Figures show the calculated PMF-values for the adsorption of the migrating component 2,6-diisopropylphenol on two polymer surfaces, i.e., cyclic olefin copolymer (Figure 4) and polypropylene (Figure 5), in different solvents. The local minimum at 1.65 nm in Figure 4 resembles the starting position. At a smaller distance the repulsion from the polymer surface leads to a drastic increase in energy. In Figure 5 there is no sharp minimum. The energy levels off in the vicinity of the polymer surface and increases only slightly. This can probably be explained with the lower density of polypropylene compared to cyclic olefin copolymer.

The error bars generated by the GROMACS utility *g_wham* are estimated using Bayesian bootstrapping. Bootstrapping is used to estimate the uncertainty of a quantity that is calculated from a large set of observations, in this case the histograms obtained from the umbrella sampling windows. The Bayesian bootstrapping technique resamples the PMF based on an estimated probability distribution underlying the histograms, assigning random weights to them.[47] Table 3 shows the obtained values for the free energy of adsorption differences between a local minimum of the curve representing the adsorbed state and the constant part of the curve where the migrating component is solely in the pure solvent.
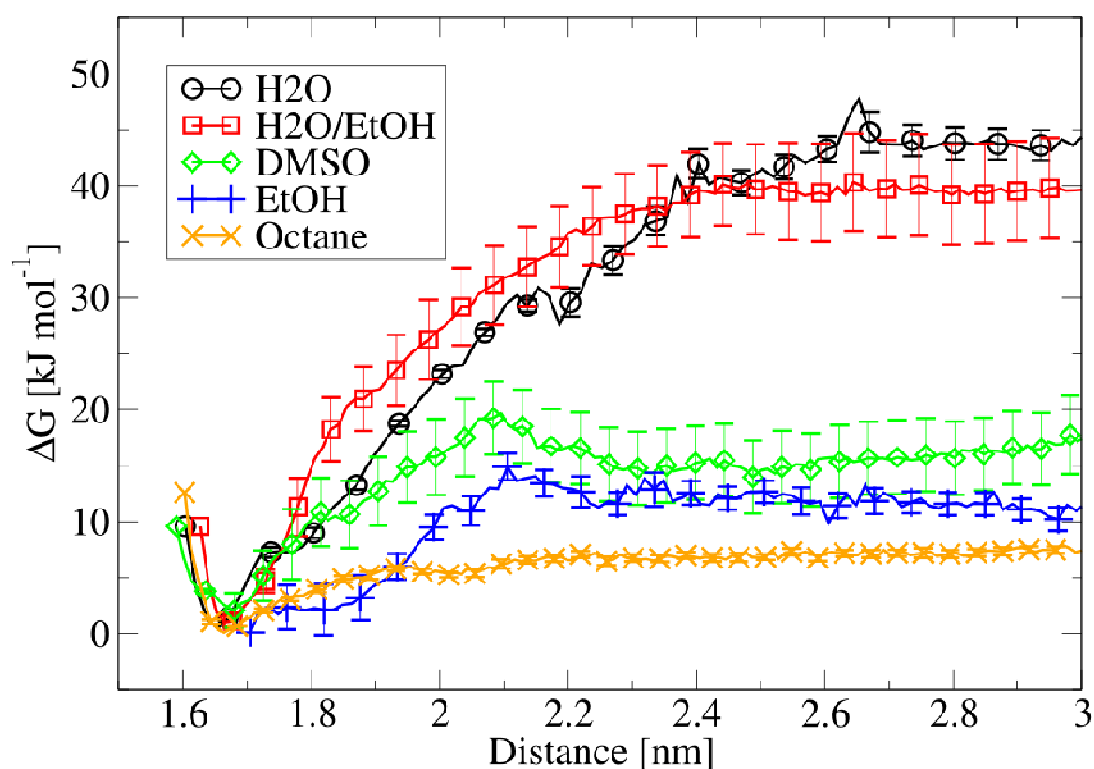
Figure 4. Potential of mean force curves for the adsorption of 2,6-diisopropylphenol on cyclic olefin copolymer in different solvents (error estimates generated using Bayesian bootstrapping)
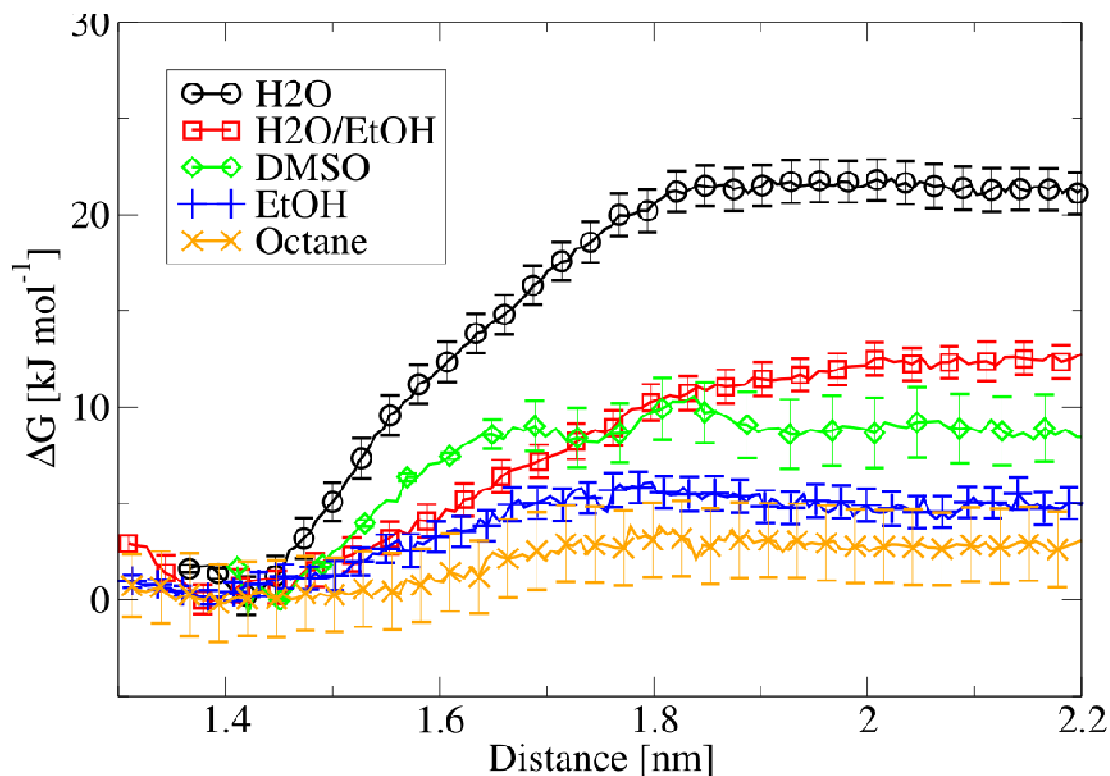

Figure 5. Potential of mean force curves for the adsorption of 2,6-diisopropylphenol on polypropylene in different solvents (error estimates generated using Bayesian bootstrapping)

Table 3 ΔG values obtained from the PMF curves for the adsorption of 2,6-diisopropylphenol on polypropylene and cyclic olefin copolymer in different solvents

Solvent	ΔG (kJ mol^{-1})	
	PP	COC
Water	43	21
Water/EtOH 50:50	38	12
DMSO	16	9
Ethanol	11	5
Octane	6	3

The PMF curves show that the behavior of the migrating component strongly depends on the solvent. As expected, the biggest energy difference was between the migrating component in water and the migrating component adsorbed to the hydrophobic surface. In contrast to the results of the LIE method, the ΔG value obtained from the PMF curve was negative, indicating favorable adsorption to the surface. For all solvents the ΔG value obtained from the PMF curve correlated with the solvent's polarity index, as reported in the literature. Figure 6 shows a plot of the ΔG values versus the polarity index of the used solvent. The polarity index for 50 v% mixture of water and ethanol was calculated according to Eq. (2):
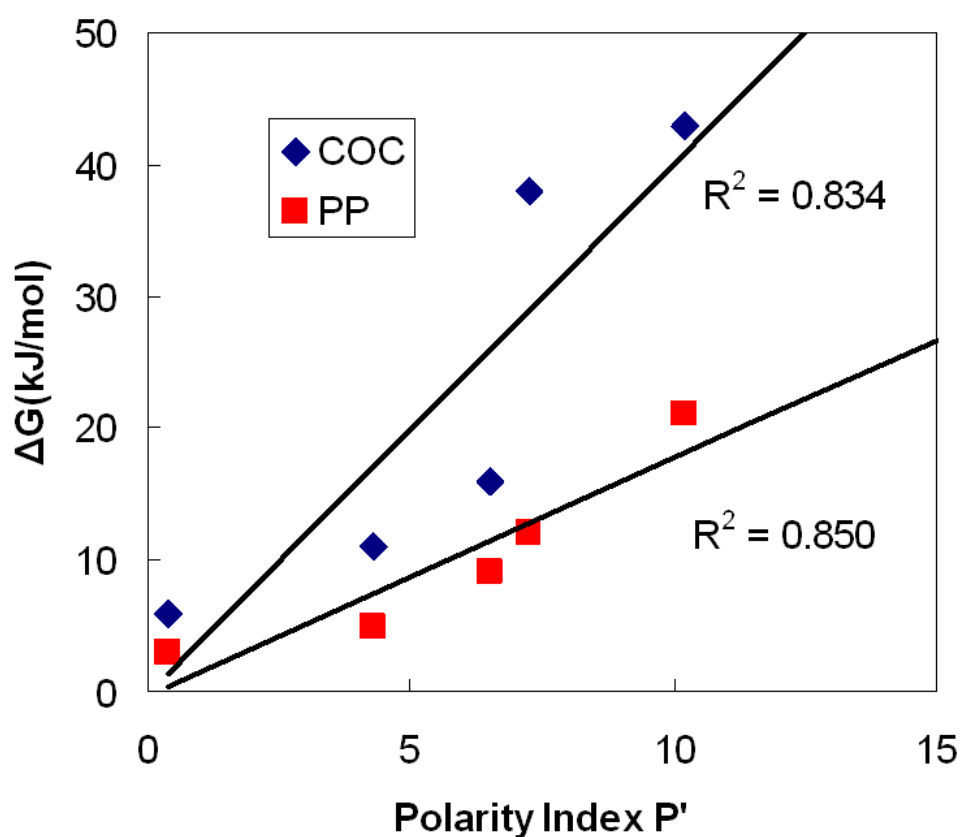
$$P'_m = \varphi \, P'_1 + (1 - \varphi)P'_2 \qquad\qquad (2)$$

where P'_m is the polarity index of the mixture and φ is the proportion (vol.) of the solvent 1 in the mixture.[2]

Table 4 shows the polarity index according to the Snyder classification of solvents.[48]

Table 4 Solvent polarity index according to Snyder [48]

Solvent	P'
Water	10.2
DMSO	6.5
Ethanol	4.3
Octanol	3.4

Figure 6. Plot of the ΔG values obtained from the potential of mean force curves vs. the polarity index

Evidently, the profiles of the plots in Figure 6 are similar, although the values for COC are proportionally higher than those for PP. A linear regression through the plotted values clearly shows a correlation between the polarity index of the solvent and the corresponding ΔG value.

To demonstrate the validity of the method for binary solvent mixtures a leaching experiment published by Jenke et al.[13] was performed as a test case. In their work Jenke et al. show that 3-(3,5-di-tert-butyl-4-hydroxyphenyl)propionic acid, leaching from a PE material accumulates in contacting solvents according to their respective polarities. A system was set up as described above and ethanol/water mixtures with an ethanol content of 15, 30 and 45 v% and water were used as solvents (see the resulting PMF curves in Figure 7). Table 5 shows the obtained values for the enthalpy differences between a local minimum of the curve representing a close vicinity to the surface and the constant part of the curve where the migrating component is solely in the pure solvent.
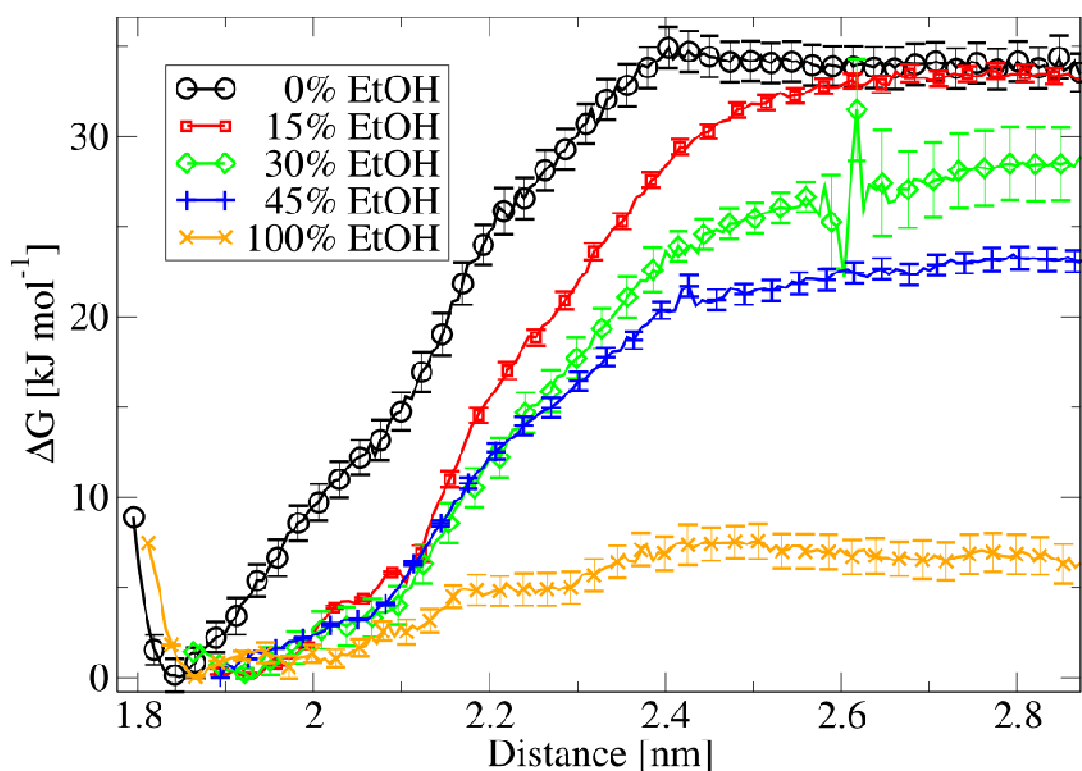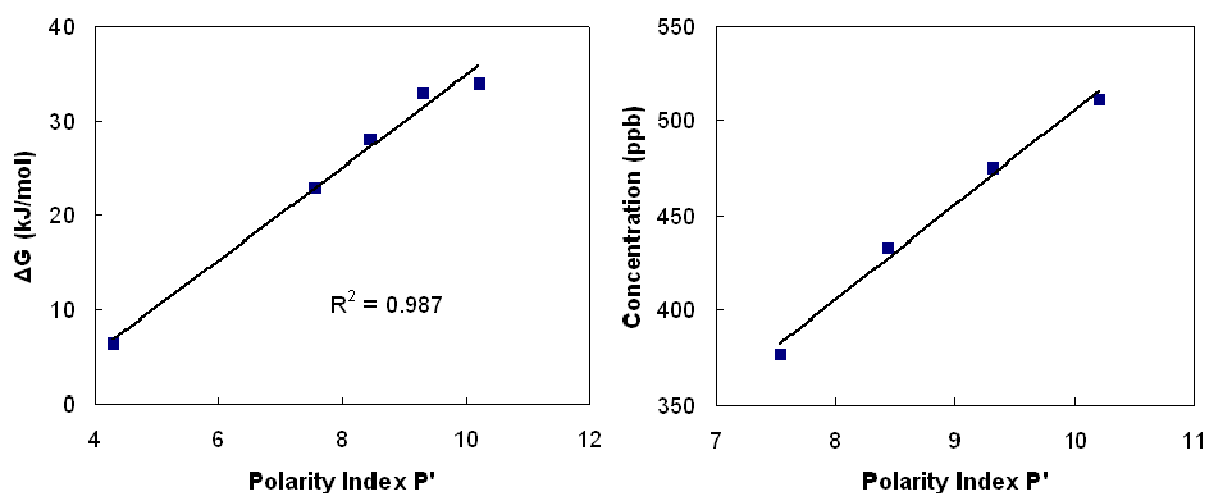

Figure 7. Potential of mean force curves for the adsorption of 3-(3,5-Di-tert-butyl-4-hydroxyphenyl)propionic acid on polyethylene in different ethanol/water mixtures

Table 5 ΔG values obtained from the PMF curves for the adsorption of 2,6-Diisopropylphenol on polypropylene in different solvents

Solvent	ΔG (kJ mol^{-1})
EtOH/water 0%	34
EtOH/water 15%	33
EtOH/water 30%	28
EtOH/water 45%	23
EtOH/water 100%	6.5

Figure 8 shows the linear correlation between the free energy of adsorption for the migrating component and the polarity of the used solvent and the experimentally determined values for the investigated system published by Jenke et al.[13] The displayed concentrations represent the amount of migrating component remaining in the polymer when the polymer was brought into contact with the respective solvent.

Figure 8. Plot of the ΔG values obtained from the potential of mean force curves vs. the polarity index (left), amount of migrating component remaining in the plastic material* (right)
*according to Jenke et al.[13]

The results indicate that the employed method can be used to predict solid-liquid interactions under the investigated conditions. The method yields semi-quantitative results for pure solvents as well as for binary mixtures. Interestingly, although the simulations were based only on the adsorption of the migrating component to the polymer surface, the resulting free energy of adsorption values correlate with the findings from leaching experiments. In reality the migrating component is also absorbed and migrates through polymeric materials. A simulation of this behavior would computationally be much more expensive since the time and length scales of such a process are far beyond the reach of state-of-the art simulation methods. Fortunately, the free energy of adsorption, which can be obtained with a reasonable computational effort, shows relative trends that stand in accordance with experimental findings published in literature. This indicates that the adsorption is a significant part of the overall migration process and the free energy contribution that relates to further migration into/out of the polymer does not depend on the used solvent.

Conclusion

The solid-liquid interactions of small organic solute molecules with polymer surfaces and common solvents were investigated using MD simulations to estimate the solvation free energy and the free energy of adsorption. The results may be summarized as follows:

(1) The investigated simulation method can be used to predict the octanol/water partition coefficient based on a calculation of the solvation free energy.

(2) The calculation of the free energy of adsorption was performed in two ways. The first one, linear interaction energy algorithm (LIE), did not yield significant differences for the binding free energy between the solute and the polymer's surface for all investigated organic solvents. For water the obtained value indicated no adsorption of the solute to the surface. This does not agree with the results obtained from direct calculations of potentials of mean force between the solute and the surface.

(3) The second approach – a direct calculation of the potential of mean force between a molecule in solution and a container wall – yielded results for the free energy of adsorption that correlate well with the polarity index of the used solvent, which agrees with published experimental results.

(4) The results furthermore indicate that, generally, MD methods and, specifically, the OPLS-AA parameters used in our study can successfully be used to investigate such solid-liquid interactions for different pure solvents as well as for binary mixtures.

(5) Although only the adsorption of solute molecules on polymers was investigated in the simulations, the results correlate with the findings from leaching experiments (the migration into/out of the polymer by either the migrating component or the solvent would in principle be possible. However, due to the small timescales examined this cannot be observed). This indicates that the contributions relating to the migration into/out of the polymer do not depend on the used solvent. Further experiments to clarify this statement are necessary.

(6) Since many drug products have a rather complex composition, simple polarity-based models for the prediction of drug packaging interactions might be insufficient. A more rigorous modeling approach, that is capable of including additional parameters, e.g., cosolvents or ionic strength, such as the method described in this work, might help overcome such difficulties.

References

[1]   D. Jenke, Compatibility of Pharmaceutical Products and Contact Materials, John Wiley & Sons, Inc., Hoboken, New Jersey, 2009.

[2]   D.R. Jenke, Int. J. Pharm. 224 (2001) 51.

[3]   E.J. Smith, in:, J. Swarbrick (Ed.), Encycl. Pharm. Technol., 3rd ed., Taylor & Francis Ltd, 2007, pp. 1466–1481.

[4]   R.G. Iacocca, M. Allgeier, J. Mater. Sci. 42 (2007) 801.

[5]   D. Jenke, J. Pharm. Sci. 96 (2007) 2566.

[6]   S. Loff, F. Kabs, K. Witt, J. Sartoris, B. Mandl, K.H. Niessen, K.L. Waag, J. Ped. Surg. 35 (2000) 1775.

[7]   E.L. Cussler, Diffusion Mass Transfer in Fluid Systems, Cambridge University Press, Cambridge, 2009.

[8]   D.R. Jenke, J.M. Jene, M. Poss, J. Story, T. Tsilipetros, A. Odufu, W. Terbush, Int. J. Pharm. 297 (2005) 120.

[9]   A. Treleano, G. Wolz, R. Brandsch, F. Welle, Int. J. Pharm. 369 (2009) 30.

[10]   M.A. Pascall, M.E. Zabik, M.J. Zabik, R.J. Hernandez, J. Agric. Food Chem. 53 (2005) 164.

[11]   D. Jenke, J. Story, R. Lalani, Int. J. Pharm. 315 (2006) 75.

[12]   O.G. Piringer, A.L. Baner, Plastic Packaging, Wiley VCH Verlag GmbH & Co. KGaA, Weinheim, 2008.

[13]   D. Jenke, A. Odufu, M. Poss, Eur. J. Pharm. Sci. 27 (2006) 133.

[14]   D.R. Jenke, J. Brennan, M. Doty, M. Poss, J. Appl. Polym. Sci. 89 (2003) 1049.

[15]   D. Hofmann, L. Fritz, J. Ulbrich, C. Schepers, M. Böhning, Macromol. Theory Simul. 9 (2000) 293.

[16]   F. MÜLLER-PLATHE, Acta Polym. 45 (n.d.) 259.

[17]   J.A. Lemkul, D.R. Bevan, J.Phys. Chem. B 114 (2010) 1652.

[18]   W.L. Jorgensen, Acc. Chem. Res. 22 (1989) 184.

[19]   J.P. Valleau, D.N. Card, J. Chem. Phys. 57 (1972) 5457.

[20]   G.M. Torrie, J.P. Valleau, J. Comput. Phys. 23 (1977) 187.

[21]   J. Aquist, C. Medina, J.E. Samuelson, Protein Eng. 7 (1994) 385.

[22]   G.M. Eccleston, Emulsions and Microemulsions, Informa Healthcare USA Inc., New York, 2007.

[23]   M.T. Baker, M. Naguib, Anesthesiology 103 (2005) 860.

[24]   D.A. Pearlman, D.A. Case, J.W. Caldwell, W.S. Ross, T.E. Cheatham III, S. DeBolt, D. Ferguson, G. Seibel, P. Kollman, Comp. Phys. Commun. 91 (1995) 1.

[25]   D.A. Case, T.E. Cheatham III, T.A. Darden, H. Gohlke, R. Luo, K.M. Merz, C. Onufriev, C.L. Simmerling, B. Wang, R. Woods, J. Comput. Chem. 26 (2005) 1668.

[26]   D.A. Case, T.A. Darden, T.E. Cheatham, C.L. Simmerling, J. Wang, R.E. Duke, R. Luo, R.C. Walker, W. Zhang, K.M. Merz, B. Roberts, B. Wang, S. Hayik, A. Roitberg, G. Seabra, I. Kolossváry, K.F. Wong, F. Paesani, J. Vanicek, X. Wu, S.R. Brozell, T. Steinbrecher, H. Gohlke, Q. Cai, X. Ye, M.-J. Hsieh, G. Cui, D.R. Roe, D.H. Mathews, M.G. Seetin, C. Sagui, V. Babin, T.

Luchko, S. Gusarov, A. Kovalenko, P.A. Kollman, Univ. California, San Fr. 11 (2010).

[27]   W.L. Jorgensen, J. Tirado-Rives, J. Am. Chem. Soc. 110 (1988) 1657.

[28]   D. van der Spoel, P.J. van Maaren, J.C. Berendsen, J. Chem. Phys. 108 (1998) 10220.

[29]   J.C. Berendsen, D. van der Spoel, R. van Drunen, Comp. Phys. Com. 91 (1995) 43.

[30]   E. Lindahl, B. Hess, D. van der Spoel, J. Mol. Mod. 7 (2001) 306.

[31]   D. van der Spoel, E. Lindahl, B. Hess, G. Groenhof, A.E. Mark, J.C. Berendsen, J. Comp. Chem. 26 (2005) 1701.

[32]   B. Hess, C. Kutzner, D. van der Spoel, E. Lindahl, J. Chem. Theory Comput. 4 (2008) 435.

[33]   U. Essmann, L. Perela, M.L. Berkowitz, T. Darden, H. Lee, L.G. Pedersen, J. Chem. Phys 103 (1995) 8577.

[34]   M. Parrinello, A. Rahman, J. Appl. Phys. 52 (1981) 7182.

[35]   W.F. van Gunsteren, J.C. Berendsen, Mol. Simul. 1 (1988) 173.

[36]   C.H. Bennett, Comp. Phys. 22 (1976) 245.

[37]   D. Wu, D.A. Kofke, J. Chem. Phys. 123 (2005) 84109.

[38]   T. Hansson, J. Marelius, J. Aquist, J. Comput. Aid. Mol. Des. 12 (1998) 27.

[39]   Y. Su, E. Gallicchio, K. Das, E. Arnold, R.M. Levy, J. Chem. Theory Comput. 3 (2007) 256.

[40]   J.Y. Shin, J.Y. Park, C. Liu, J. He, S.C. Kim, Pure Appl. Chem. 5 (2005) 801.

[41]   J.C. Berendsen, J.P.M. Postma, W.F. van Gunsteren, A. DiNola, J.R. Haak, J. Chem. Phys. 81 (1984) 3684.

[42]   G. Bussi, D. Donadio, M. Parrinello, J. Chem. Phys. 126 (2007) 14101.

[43]   J.E. Mark, Polymer Data Handbook, Oxford University Press, Oxford, 1999.

[44]   R.R. Lamonte, D. McNally, Adv. Mater. Process. 159 (2001) 33.

[45]   I.G. Tironi, R. Sperb, P.E. Smith, W.F. van Gunsteren, J. Chem. Phys. 102 (1995) 5451.

[46]   A.M. Evans, B.L. Holian, J. Chem. Phys. 85 (1983) 4069.

[47]   J.S. Hub, B.L. de Groot, D. van der Spoel, J.Chem. Theory Comput. 6 (2010) 3713.

[48]   L.R. Snyder, J. Chromatogr. 92 (1974) 223.

Investigation of Migrant – Polymer Interaction in Pharmaceutical Packaging Material using the LIE Algorithm[5]
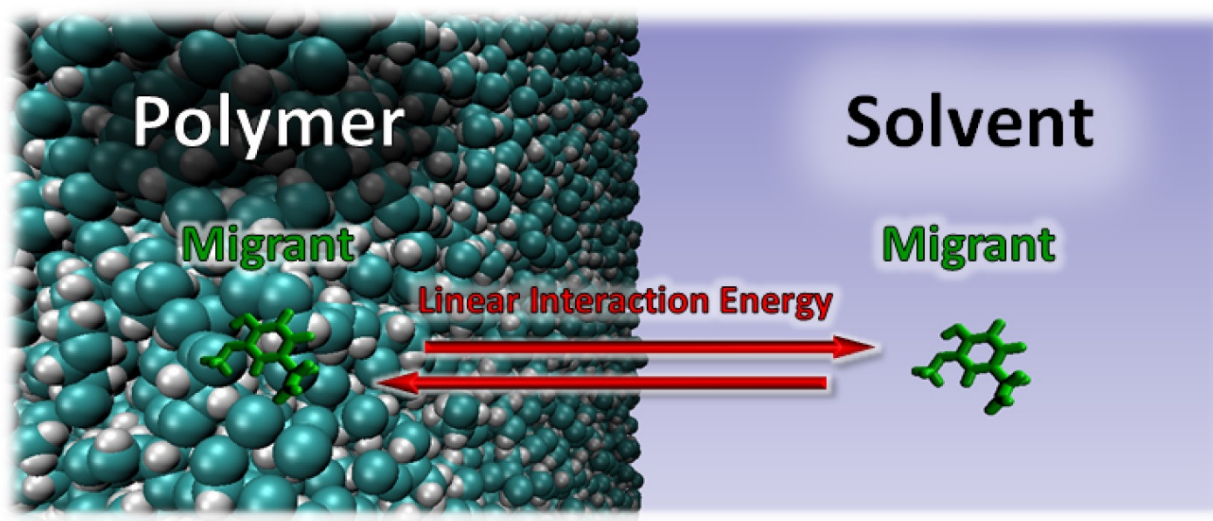
The interaction between drug products and polymeric packaging materials is an important topic in the pharmaceutical industry and often associated with high costs due to the required elaborative interaction studies. Therefore, a theoretical prediction of such interactions would be beneficial. Often material parameters such as the octanol water partition coefficient are used to predict the partitioning of migrant molecules between a solvent and a polymeric packaging material. Here we present the investigation of the partitioning of various migrant molecules between polymers and solvents using molecular dynamics simulations for the calculation of interaction energies. Our results show that the use of a model for the interaction between the migrant and the polymer at atomistic detail can yield significantly better results when predicting the polymer solvent partitioning than a model based on the octanol water partition coefficient.

---

[5] This chapter is taken from a Journal article by Feenstra et al. in the Journal of Pharmaceutical Sciences (2014)

Introduction

Polymers are ubiquitously used in the food and pharmaceutical industry as packaging materials or process aids. Therefore, during their production, shipment and storage, the exposure of pharmaceutical products to various polymers is common.[1,2] Every such exposure bears the risk of undesired migration of compounds present in either the drug product or the polymer. Consequently, adverse safety effects cannot be excluded.[3,4] The mass transport of migrants (and possible reaction) between the polymer and the drug product are usually classified as leaching and sorption. Leaching describes the process of migration from the polymer into the drug product, while sorption describes the inverse process, i.e., when a migrant, such as an active pharmaceutical ingredient (API), moves into the polymer.[5] Sorption is further divided into (i) adsorption (accumulation of a migrant at the surface of the polymer), (ii) absorption (dispersion of a migrant in the polymer) and (iii) permeation (transition of a migrant through the polymer).[6]

Especially in the pharmaceutical industry, the experimental analysis of possible adverse interactions can lead to significant costs due to the rigorous regulatory requirements and the fact that with the increasing complexity of drug products (e.g., emulsions with various additives, such as stabilizers, etc.) the analysis of the migrants' interaction between a drug product and polymers is not straightforward. A method to overcome these problems is to perform experiments not with the actual complex drug product but with a simplified (simulated) product.[4] From the corresponding experimental data, when combined with heuristic rules, mathematical models of migrant – polymer interactions can be established with the main goal of predicting the mass transport of the migrant between the drug product and the polymer. The mass transport itself can be described by two main parameters: the partition and the diffusion coefficient.[7] Partition and diffusion coefficients are determined by the physical and chemical natures of the (simulated) drug product, the migrant and the polymer, as well as the migrant's concentration, the environmental temperature and the contact time of the system.[8,9]

One established parameter for the prediction of migrant transport (e.g., cell membrane transition by a drug molecule) is the octanol/water partition coefficient $P_{o/w}$.[10–12] It is defined as the ratio of the equilibrium concentrations of a specific

migrant in octanol (C_o) and water (C_w), Eq. (1). A similar property is the equilibrium interaction constant E_b that describes the ratio of the equilibrium concentrations of a migrant in the polymer (C_p) and the adjacent solvent (C_s), Eq. (2).

$$P_{o/w} = \frac{C_o}{C_w} \qquad (1)$$

$$E_b = \frac{C_p}{C_s} \qquad (2)$$

According to Jenke [13] the log E_b correlates linearly with the log $P_{o/w}$ as denoted in Eq. (3) with regression constants for the individual polymer. Moreover, it also linearly correlates with the polarity of the solvent P_m, Eq. (4).[5,14]

$$\log E_b = a \times (\log P_{o/w}) + b \qquad (3)$$

$$\log E_b \propto P_m \qquad (4)$$

Ideally, these relationships should allow the prediction of the equilibrium concentration of a migrant in either the drug product or the polymer based on the materials' properties and the initial concentrations.

Since both properties, $P_{o/w}$ and E_b, are determined by the molecular structures of and the intermolecular forces between the involved molecules a more sophisticated investigation of the migrant's behavior should be based on microscopic or atomistic properties. Microscopic properties can be the structural parameters like polymer chain length, chain segment angles, averaged distance between chains, migrant collision diameters, etc., while sophisticated atomistic models use very elementary physical-chemical data. These methods are capable of producing remarkable results but they require powerful computers, appropriate software and a good model parameterization.[7,15] For example, molecular dynamics (MD) simulations are widely used in the field of biochemistry and material sciences [16,17] as well as in pharmaceutical sciences.[15,18–22]

In recent studies [23] we demonstrated the applicability of MD simulations for the investigation of leaching and sorption processes. We used different approaches to evaluate the applicability of MD simulations towards the investigation of leaching and sorption processes like the calculation of the solvation free energy $\Delta_{solv}G$ [24], the potentials of mean force (PMF) between a molecule in solution and a container wall [25,26] and the linear interaction energy algorithm (LIE).[27]

Most applications of the LIE algorithm are found in the estimation of relative protein-ligand binding affinities.[28,29] It is computationally less expensive than other computational methods, such as thermodynamic integration or free energy perturbation, because it requires only two MD simulations for each investigated system: one with the migrating component in solution (free state) and the other with the migrating component bound to the polymer (bound state). More importantly, with current algorithms/methodologies the direct application of thermodynamic integration or free energy perturbation is not possible for solid solvents, such as PVC at ambient conditions, while the application of LIE is comparatively straightforward. The electrostatic and van der Waals interactions in the free and in the bound state are computed and the binding free energy can be estimated by a linear combination of these values.[28,30,31] Therefore, the LIE method promises to be a valuable tool for the investigation and prediction of migrant-polymer interactions in analogy to protein-ligand interactions.

Here we apply the LIE method to the prediction of the migration of small, drug-like molecules between a polymer and a solvent and compare the results with those predicted with a log $P_{o/w}$ to log E_b relation. The used molecules show various chemical structural motifs and diverse log $P_{o/w}$ values. The polymers used in this study were polyethylene (PE) and polyvinylchloride (PVC), which are commonly used in packaging materials in the pharmaceutical industry.

Methods

For our simulations all components were manually sketched using the AMBER [32–34] module xleap. The corresponding OPLS-AA [35] (Optimized Potentials for Liquid Simulations – All Atoms) force field parameters (including charge) were applied to all atoms. When required, small manual adjustments were made to partial charges to ensure that the molecules net-charge was zero. The topology files can be found in the Supporting Information. All MD simulations were performed using the GROMACS [36–39] software package version 4.5.3. VMD 1.8.7 [40] was used to visually analyze the investigated systems.

For the calculation of the migrant-solvent interaction systems 3 migrant molecules were put inside a cubic box with the side length of 4 nm followed by solvation with the solvent at ambient density. Periodic boundary conditions were applied and van der Waals interactions were cut off at 1.4 nm. Long-range electrostatics was accounted for using particle mesh Ewald.[41] The box was equilibrated at the temperature of 300 K using a Nosé-Hoover thermostat.[42] The pressure of 1 bar was held constant by a Berendsen barostat with a time constant of 0.5 ps and compressibility of 4.5×10^{-5} bar^{-1}.[43] 5,000 steps of steepest descent minimization were followed by 100,000 steps of equilibration. The equations of motion were solved using a time step of 2 fs. Production runs for the LIE calculations spanning 1 ns of simulation time were performed for each migrant molecule – solvent pair.

Initial structures for the systems containing the migrant immersed in the packaging material were generated as follows: Starting coordinates for the polymeric packaging material (polyvinylchloride and polyethylene) were generated in such a way that the polymeric chains were aligned along the z-axis. Via this procedure, a PVC chain with a molecular weight of 25 kDa and a PE chain with a molecular weight of 19 kDa were generated. Then 3 molecules of the migrant molecule were added to the system and randomly placed in the simulation box. Initially periodic boundary conditions were applied only in the x- and y-directions. In the z-direction walls were used to simulate a "die casting" process, where the system was compressed in the z-direction at a pressure of 1,000 bar and a temperature of 600 K. Due to the resulting large forces a time step of 1 fs had to be used during compression to ensure stability of the system. Temperature was controlled using a Berendsen

thermostat.[43] After equilibration for 1 ns at the elevated pressure and temperature the system was brought to ambient conditions (300 K, 1 bar) and re-equilibrated for 1 ns to reach a final conformation of the entangled polymer chain inside the cubic box with a side length of approximately 3 nm. The final densities, 1,330 kg/m³ for PVC and 900 kg/m³ for PE, are close to experimental values.[44] The final coordinates were used as a starting conformation for the migrant-polymer production runs, again 1 ns of simulation time for each migrant molecule – polymer pair. Interaction energies between the migrant and the polymer and between the migrant and the solvent were analyzed using the GROMACS utility *g_lie*.

This way LIE values for the migrating component inside the two polymers (PVC and PE) representing the "bound state" were calculated. The LIE values for the "free state," in which the migrating component was dissolved in a pure solvent, were calculated as well.

The difference in the free energy values for the two states is then defined as ΔG_{bind} (Eq. 5).[28]

$$\Delta G_{bind} = \alpha_{polymer} \left\langle V_{l-s}^{vdW} \right\rangle_{bound} - \alpha_{solvent} \left\langle V_{l-s}^{vdW} \right\rangle_{free} + \beta_{polymer} \left\langle V_{l-s}^{el} \right\rangle_{bound} - \beta_{solvent} \left\langle V_{l-s}^{el} \right\rangle_{free} \qquad (5)$$

‹V› denotes the simulation average of the non-bonded potential energy between ligand (subscript "l", in this case the migrant molecule) and surrounding (subscript "s", a polymer or solvent). α and β are the scaling factors for van der Waals and electrostatic interactions between the migrant and its surroundings. The individual α and β values can be adjusted using empirical data.[28] In this work no such adjustment was performed and the parameters proposed in the original publication (α = 0.181, β = 0.5) [27] were used.

A validation run in which the migrant molecules were placed differently during the compression phase resulting in differing starting conformations was performed in one case and yielded no significant differences in the resulting LIE values. This way we assured that the number of samples (starting conformations) in the polymer is sufficient to yield a representative average value. The enthalpy values for the migrant molecules are composed of all electrostatic and van der Waals interactions between the migrants and its environment. Those were also taken from the LIE production runs.

For the calculation of the free energy of solvation the migrating component was put inside a cubic box with the side length of 3.5 nm followed by solvation with the appropriate solvent at ambient density. Periodic boundary conditions were applied and all distance-dependent properties were cut off at 1.15 nm. Long-range electrostatics was accounted for using particle mesh Ewald.[41] The box was equilibrated at the temperature of 298 K. The pressure of 1 bar was held constant by a Berendsen barostat [43] with a compressibility of 10^{-5} bar^{-1}. The equations of motion were solved using an sd integrator [45] with a time step of 2 fs. Production runs for the calculations of free energies of solvation were performed at the following λ-values: {0.0/0.0, 0.2/0.0, 0.5/0.0, 1.0/0.0, 1.0/0.2, 1.0/0.4, 1.0/0.6, 1.0/0.8, 1.0/1.0} Here, λ denotes the coupling parameter describing interactions between the solute and the solvent with the first value being for coulomb interactions and the second value being for van der Waals interactions. At $\lambda = 0$ all interactions were switched on and at the value of $\lambda = 1$ all interactions were switched off. In water and methanol production runs of 1 ns simulation time each were performed. In octanol production runs were performed for 400 ps but 6 different random starting conformations were used per molecule. The larger molecule size of octanol greatly increases the equilibration time and this way a more representative sampling can be guaranteed in octanol The ΔG_{solv} values were calculated using the multistate Bennett acceptance ratio estimator 'MBAR'. [46]
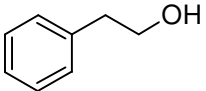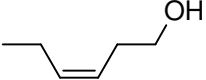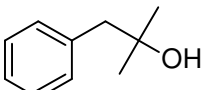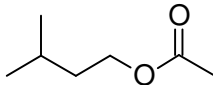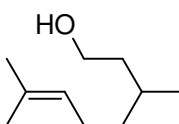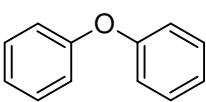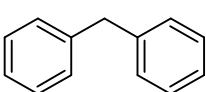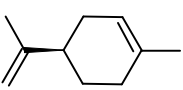
Results and Discussion
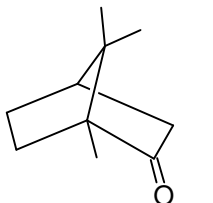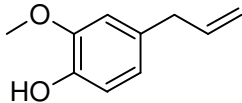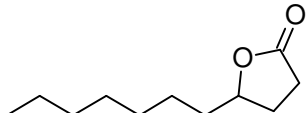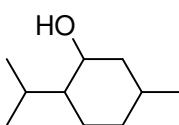
The migrant molecules used for the LIE calculations are 2-phenylethylalcohol (**1**), 3-hexenol (**2**), dimethylbenzylcarbinol (**3**), isoamylacetate (**4**), camphor (**5**), eugenol (**6**), γ-undecalacton (**7**), menthol (**8**), citronellol (**9**), diphenyloxide (**10**), diphenylmethane (**11**) and limonene (**12**). Their chemical structures, as well as their log $P_{o/w}$ and log E_b values, are depicted in

Table. All molecules are aroma compounds and their partitioning behavior between various combinations of polymers and solvents was studied and published by Piringer and Baner.[7]

We are aware that the chosen molecules are neither used as active pharmaceutical ingredients nor are they found as additives in polymer packaging. Nevertheless, the molecules comply well with Lipinski's rule of five for druglikeness. They were chosen because on one hand they have rather similar molecular weights while on the other hand they show various different chemical structural motifs that are indeed found in active pharmaceutical ingredients as well as in polymer additives. Moreover, their diverse log $P_{o/w}$ values make them a valuable test set for a general proof of principle of the applied method. The polymers used in this study were polyethylene (PE) and polyvinylchloride (PVC). PE and PVC are commonly used in packaging materials in the pharmaceutical industry and are composed of ethylene and vinylchloride monomeric units, respectively. The solvent considered was methanol. Though methanol is not extensively used in pharmaceutical formulations it can be used to mimic a complex drug product based on its solvent polarity (polarity index 6.6) that lies between those of a non-polar environment (e.g. octanol, polarity index: 3.2) and a purely aqueous environment (polarity index 9).[13,47] Again, the solvent choice was made out of practical reasons to proof the principal applicability of the method. For every migrant molecule listed in Table 1 three simulations were performed, lasting one nanosecond of simulation time each; one with the migrant in the PE environment, one in the PVC environment and one in the methanol environment.

Table 1. log $P_{o/w}$ and log E_b values for various migrant molecules for the systems polyethylene (PE) – methanol and polyvinylchloride (PVC) – methanol (data reported by Piringer and Baner [7])

Entry	Chemical Formula	log $P_{o/w}$	log $E_{b,PE}$	log $E_{b,PVC}$
1		1.46	-2.15	-0.72
2		1.53	-2.52	-0.96
3		1.86	-1.92	-0.82

Entry	Chemical Formula	log $P_{o/w}$	log $E_{b,PE}$	log $E_{b,PVC}$
4		2.24	-1.37	-0.29
5		2.26	-1.15	-0.68
6		2.39	-1.70	-0.40
7		3.20	-1.37	-0.02
8		3.20	-1.85	-1.60
9		3.41	-1.74	-1.08
10		4.04	-0.64	0.26
11		4.28	-0.57	0.34
12		4.54	-0.13	-

According to Eq. (3) a prediction of the log E_b values based on known log $P_{o/w}$ values is possible. For an evaluation of this prediction method we consider the correlations between log E_b and log $P_{o/w}$ values as shown in Figure 1 and Figure 2.
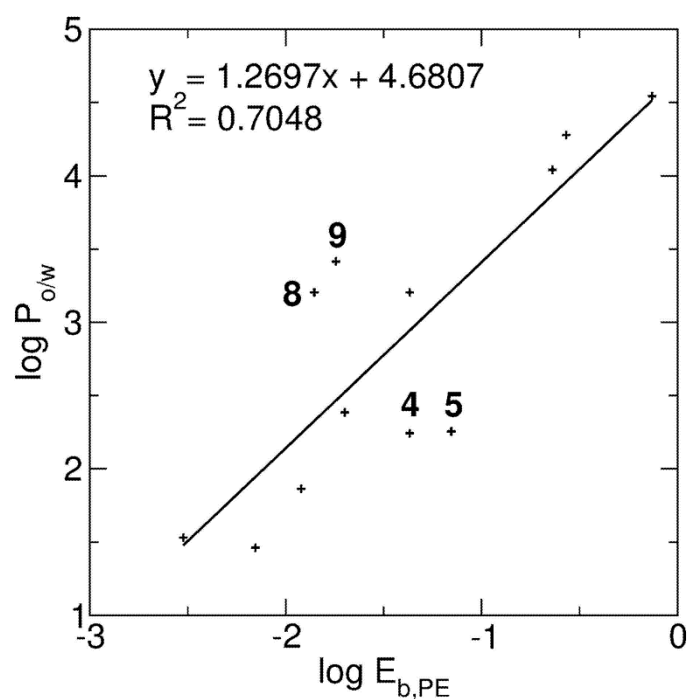
Figure 1. Correlation between log $P_{o/w}$ and log E_b for migrant molecules (E_b values for the system PE – methanol)
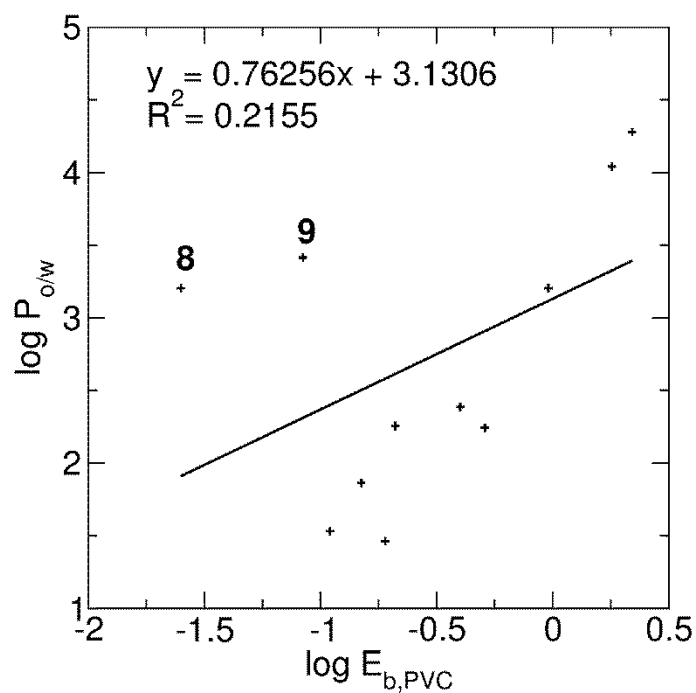

Figure 2. Correlation between log $P_{o/w}$ and log E_b for migrant molecules (E_b values for the system PVC – methanol)

As can be clearly seen, there are strong outliers (most conspicuous the entries **8** and **9** for both systems as well as entries **4** and **5** for the system PE - methanol). Due to

these outliers the resulting correlations are relatively poor, in particular for PVC. The correlation coefficient R^2 for the system PE – methanol is 0.70 and for PVC – methanol only 0.22.

For the comparison of this prediction with a more rigorous method we approximate the free energy difference between the migrant molecules in the polymer and in methanol using the LIE algorithm. Following a variation of the Gibbs-Helmholtz equation that relates the reaction free enthalpy ($\Delta_r G^O$) to the equilibrium constant K (Eq. (6)), one can assume that the "reaction free enthalpy" of binding of a molecule to a polymer (ΔG_{bind}) is equivalently proportional to the logarithmic value of the equilibrium interaction constant $E_b = C_p/C_s$.

$$- \Delta_r G^\circ = RT \ \ln K \qquad (6)$$

$$-\Delta G_{bind} \propto \ln E_b \qquad (7)$$

The results for the binding free energy obtained from the LIE calculations for the system PE – methanol and PVC – methanol are displayed in Table 2. The values are presented as the negative values $-\Delta G_{bind}$ so that they are directly proportional to E_b.

Table 2. Calculated values for the binding free energy $-\Delta G_{bind}$ of different migrant molecules between methanol and PE as well as methanol and PVC

	$-\Delta G_{bind}$ (kJ/mol)					
Entry	PE			PVC		
1	-22.87	+/-	0.49	-12.94	+/-	2.16
2	-21.24	+/-	0.91	-13.96	+/-	1.47
3	-23.43	+/-	0.99	-13.49	+/-	1.48
4	-4.37	+/-	0.90	-1.16	+/-	1.70
5	-7.06	+/-	1.12	0.52	+/-	1.16

Entry	-ΔG$_{bind}$ (kJ/mol)					
	PE			PVC		
6	-16.96	+/-	1.36	-4.72	+/-	1.21
7	-10.15	+/-	0.45	2.47	+/-	1.92
8	-18.46	+/-	1.90	-10.11	+/-	2.86
9	-20.73	+/-	0.38	-10.58	+/-	1.64
10	-8.14	+/-	1.85	2.25	+/-	1.96
11	-3.16	+/-	0.27	3.85	+/-	1.76
12	2.68	+/-	0.31	-	+/-	-

Figure 3 and Figure 4 display the plot of the -ΔG$_{bind}$ values versus the log E$_b$ values. Though not ideal, the correlation is significantly better than the one between log E$_b$ and log P$_{o/w}$.
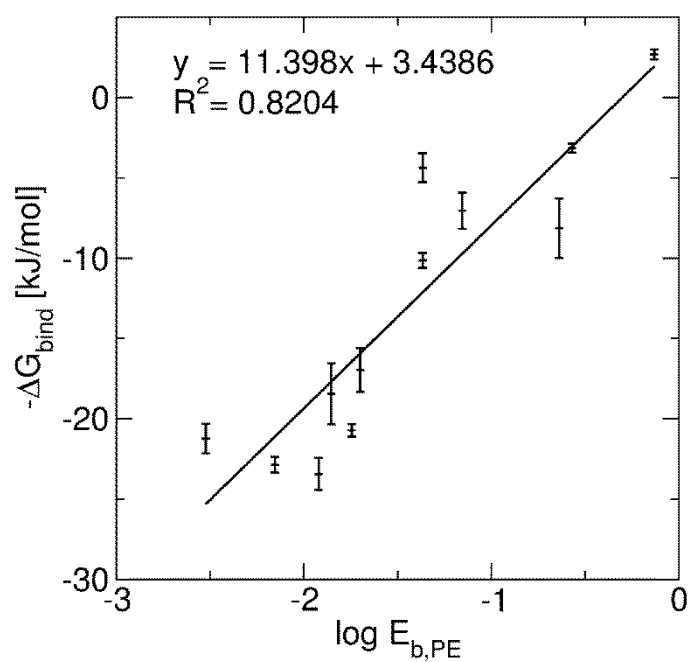

Figure 3. Correlation between log E$_b$ and -ΔG$_{bind}$ for the system PE – methanol
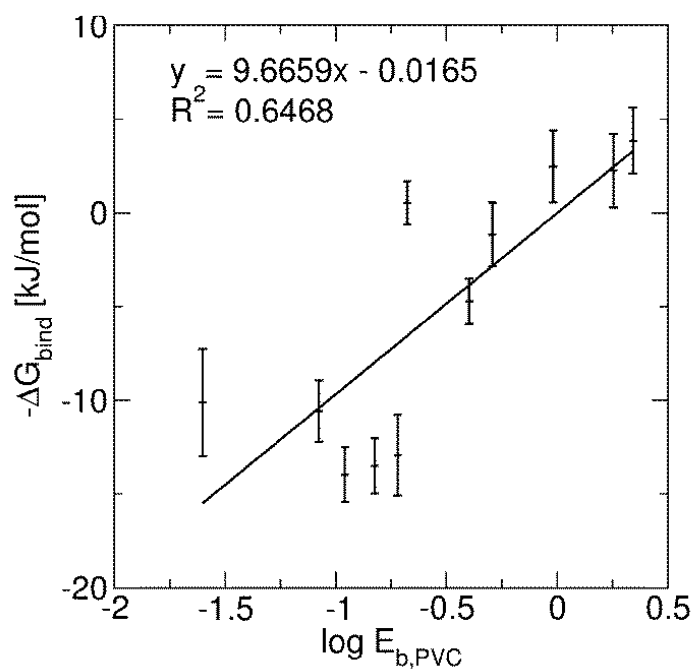
Figure 4. Correlation between log E_b and $-\Delta G_{bind}$ for the system PVC – methanol

Combining the results for both polymer – methanol systems and plotting the log E_b values vs. the $-\Delta G_{bind}$ values still yields a linear correlation as shown in Figure 5.
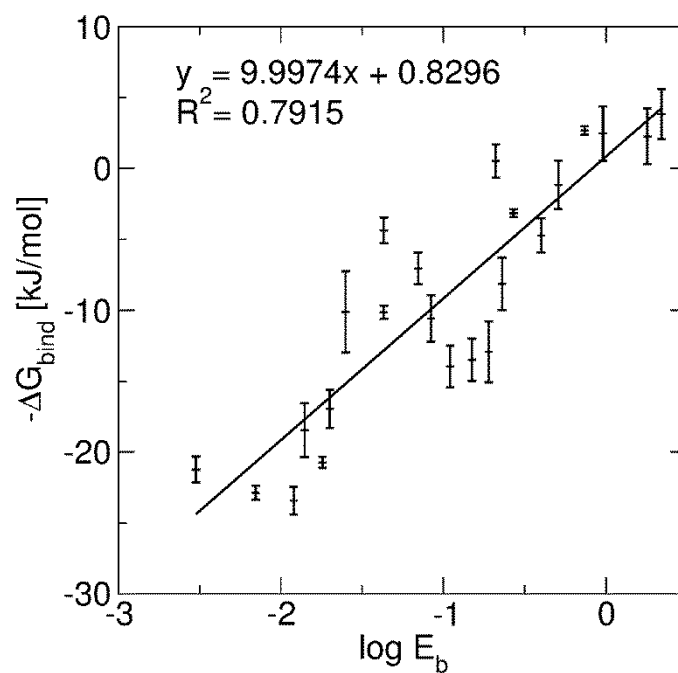

Figure 5. Correlation between log E_b and $-\Delta G_{bind}$ for both polymer – methanol systems

A linear regression of the correlation shown in Figure 5 yields a correlation coefficient of 0.79 for the LIE method for both investigated polymer – solvent systems. Consequently, this means that a prediction of the polymer-solvent partitioning of the investigated migrant molecules based on the $-\Delta G_{bind}$ values obtained by the LIE calculations yields a better result than a prediction using Eq. (3). Notably, compared to the log $P_{o/w}$ method where regression constants have to be used for each individual polymer, the LIE based method does not need such a scaling for the investigated systems

The LIE method works with rather gross simplifications especially when it comes to entropic contributions to the ΔG_{bind} values. Therefore, it is often used for the comparison of rather similar ligand-protein binding interactions where the change in entropy between the compared cases is small or of comparable magnitude so that they cancel out when we are only interested in correlations, i.e. relative rather than absolute free energies. Here, the differences between the entropic contributions should be large when comparing a rather rigid molecule like limonene (**12**) with a flexible molecule like γ-undecalacton (**7**). Nevertheless, the LIE method performs well for the investigated cases.

To investigate the reasons for the good correlations obtained we performed rigorous free energy calculations for all migrant molecules in water, methanol and octanol. The results indicate that for the solvent used in this study (methanol) the free energy of the migrant molecules in solution and the corresponding enthalpic contributions show a good correlation, suggesting that the enthalpic contributions to the free energy stemming from the interactions of functional groups between the migrant molecules and the surrounding phase dominate while the entropic contributions are of comparable magnitude and cancel out. Figure 6 shows the correlation between free energy and enthalpy of the migrants in methanol.
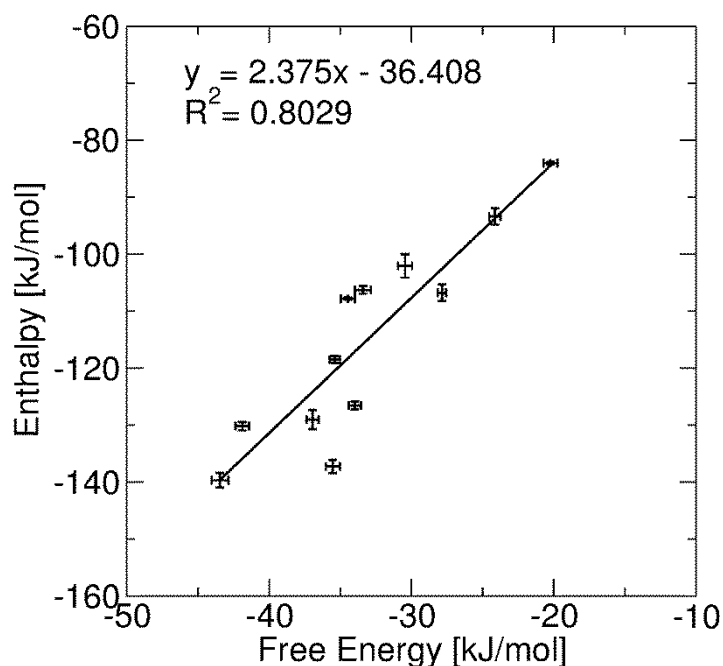
Figure 6. Correlation between enthalpy and free energy for the migrant molecules in methanol

A comparison of calculated free energy and enthalpy values for the polymer phases has not been performed here as free energy calculations in solid amorphous phases at ambient conditions are not feasible with established computational algorithms.[48] Figure 7a shows the comparison of the free energy values between methanol and octanol and Figure 7b shows the comparison of the enthalpy values between methanol and octanol. It is clearly visible that the free energy as well as the enthalpy values correlate well for both environments.
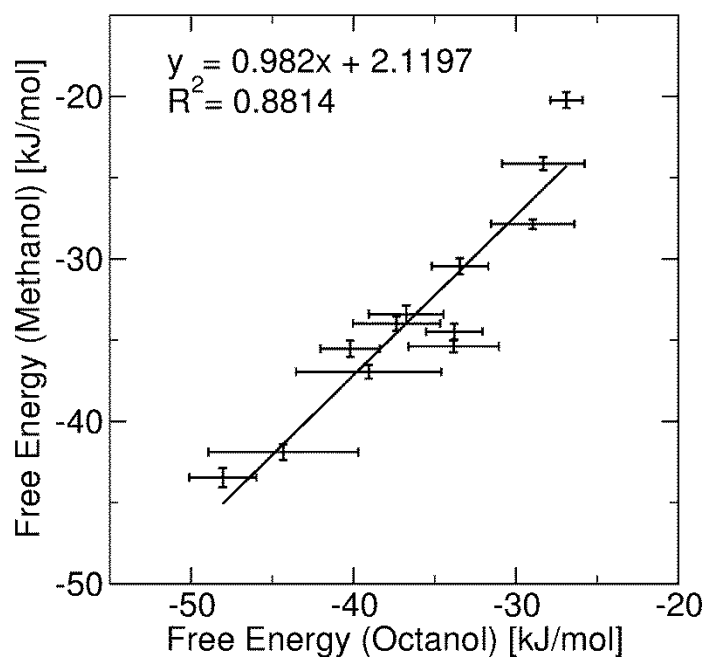
Figure 7a. Correlation between the free energy of the migrant molecules in octanol and methanol
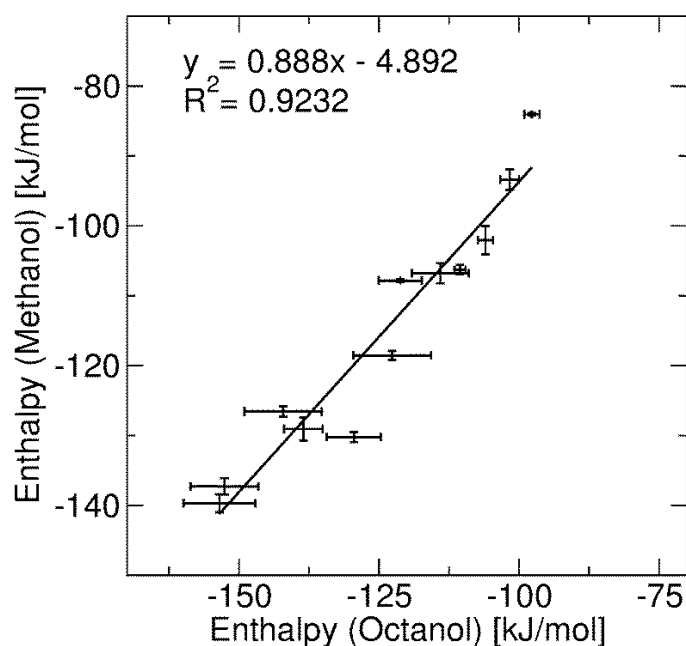
Figure 7b. Correlation between the enthalpy of the migrant molecules in octanol and methanol

In contrast, a change from an aqueous environment to an organic environment comes with specific changes in free energy that are significantly different from the changes occurring between two organic phases. The interactions of a migrant in octanol and water which forms the basis for the $\log P_{o/w}$ method are substantially different from those in a polymer and an organic solvent. Major differences are the

lack of hydrogen bond formation in polymers compared to octanol as well as a higher emphasis for entropic contributions in aqueous systems.

To explain why certain molecules (especially molecules 8 and 9) do not follow a behavior predicted by the $\log P_{o/w}$ method while the LIE method yields better correlations for these cases we have to look at their free energy of solvation in water and octanol as shown in Figure 8. The free energy of solvation in water for the molecules 8 and 9 is significantly more positive than for all other regarded alcohols while their free energy of solvation in octanol is in the same range as for the other alcohols. This means that the relatively high $\log P_{o/w}$ value for molecules 8 and 9 stems mainly from their poor interaction with water.
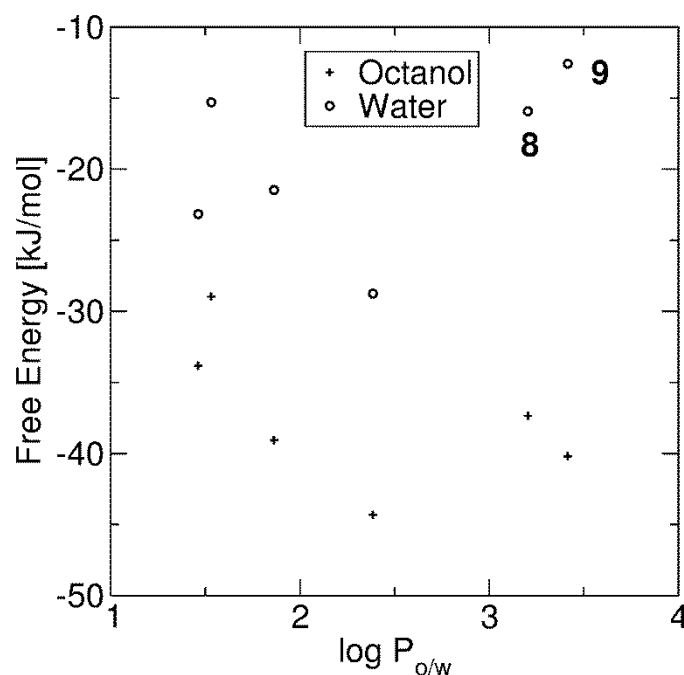
Figure 8. Free energy contributions from octanol and water to the $\log P_{o/w}$ values for the different alcohols

Since $\log P_{o/w}$ based methods are still frequently used in pharmaceutical sciences to predict the partitioning of migrants in various systems it is a major result of this work that one cannot assume that the $\log P_{o/w}$ method will accurately predict the interactions between a polymer and an organic solvent.

An important aspect of a computational prediction method is the computational demand required to obtain converged and reproducible results. Figure 9 shows the

convergence of the ΔG_{free} value for the system limonene (**12**) in methanol. The plot shows the average ΔG_{free} value of three migrant molecules versus the simulation time and also displays the standard deviation. It can be seen that a constant value is reached after about 300 ps and changes in the standard deviation become insignificant after 800 ps. Among the investigated molecules limonene is a rather compact and rigid molecule; therefore, a fast convergence of its ΔG value can be expected. In contrast, γ-undecalacton (**7**) is a long-stretched flexible molecule increasing the time for the convergence of the ΔG value. In Figure 10 the average ΔG_{bound} value of three migrant molecules for the system γ-undecalacton in PE is shown. As can be seen, a constant value is reached at about 1 ns while the standard deviation does not decrease further after this point. Considering that γ-undecalacton is a "complicated" molecule considering the convergence of its ΔG value, a simulation time of 1 ns for the investigation of the individual systems does not seem excessive. A 1-ns run corresponds to approximately 5 h of computational wall time on a state of the art desktop computer with a 2.0 GHz quadcore CPU. Thus, based on this method, pharmaceutical packaging systems can be designed in a more quantitative and sophisticated manner with moderate computational effort.
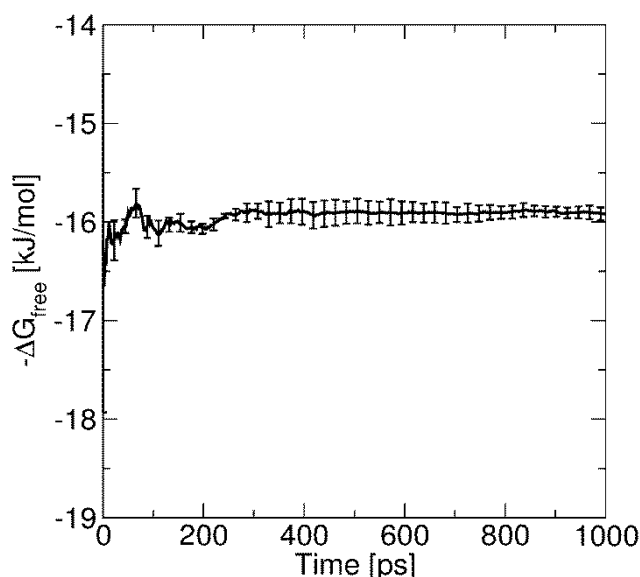

Figure 9. Time dependent change of ΔG_{free} for limonene in methanol
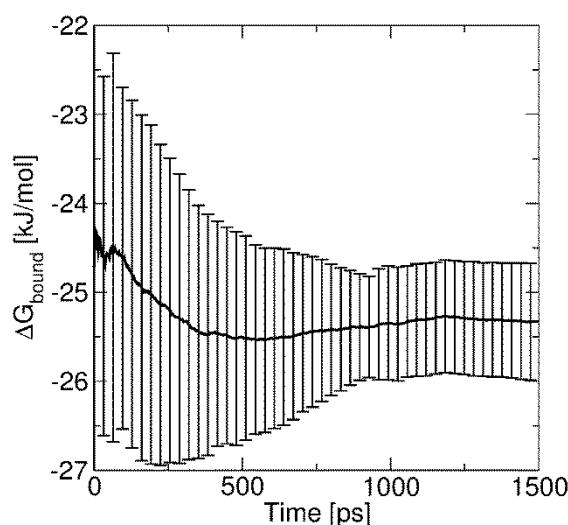
Figure 10. Time dependent change of ΔG_{bound} for γ-undecalacton in PE

Conclusion

It was shown that the use of molecular dynamics (MD) simulations for the calculation of the linear interaction energy (LIE) between a migrant and a polymer and solvent is a suitable approach for the prediction of the polymer – solvent partitioning behavior of the migrant. For the test set used here we find that the detailed model of the polymer and the migrant molecule is capable of incorporating interactions that are not accounted for by a model based on the octanol/water partitioning coefficient ($P_{o/w}$) of the migrant. Therefore, the used model is able to predict the behavior of two migrants better than a $P_{o/w}$ based model. This is the case because the solvent phase used in this study was a polar organic solvent (methanol) as a substitute for a non-aqueous system rather than water. Furthermore, the comparison of the results for two different polymers showed that the calculated LIE values correlated well with experimental partitioning data without the need for an additional fit of parameters for the individual polymers. At least for the two test cases considered the method is capable of predicting the partitioning behavior of different migrant molecules in a polymer – solvent system with a higher accuracy than a log $P_{o/w}$ based method. As a consequence this method can be the basis for the rational design of pharmaceutical packaging materials and systems when dealing with non-aqueous drug products.

References

[1]   D.R. Jenke, J.M. Jene, M. Poss, J. Story, T. Tsilipetros, A. Odufu, W. Terbush, Int. J. Pharm. 297 (2005) 120.

[2]   D. Jenke, J. Pharm. Sci. 96 (2007) 2566.

[3]   S. Loff, F. Kabs, K. Witt, J. Sartoris, B. Mandl, K.H. Niessen, K.L. Waag, J. Ped. Surg. 35 (2000) 1775.

[4]   D. Jenke, Compatibility of Pharmaceutical Products and Contact Materials, John Wiley & Sons, Inc., Hoboken, New Jersey, 2009.

[5]   D.R. Jenke, Int. J. Pharm. 224 (2001) 51.

[6]   E.J. Smith, in:, J. Swarbrick (Ed.), Encycl. Pharm. Technol., 3rd ed., Taylor & Francis Ltd, 2007, pp. 1466–1481.

[7]   O.G. Piringer, A.L. Baner, Plastic Packaging, Wiley VCH Verlag GmbH & Co. KGaA, Weinheim, 2008.

[8]   M.A. Pascall, M.E. Zabik, M.J. Zabik, R.J. Hernandez, J. Agric. Food Chem. 53 (2005) 164.

[9]   M.C. Wenlock, P. Barton, Mol. Pharm. 10 (2013) 1224.

[10]   G. Eugene Kellogg, D.J. Abraham, Eur. J. Med. Chem. 35 (2000) 651.

[11]   O.A. Santos-Filho, A.J. Hopfinger, T. Zheng, Mol. Pharm. 1 (2004) 466.

[12]   A.C. Chamberlin, D.G. Levitt, C.J. Cramer, D.G. Truhlar, Mol. Pharm. 5 (2008) 1064.

[13]   D. Jenke, A. Odufu, M. Poss, Eur. J. Pharm. Sci. 27 (2006) 133.

[14]   D.R. Jenke, J. Brennan, M. Doty, M. Poss, J. Appl. Polym. Sci. 89 (2003)
       1049.

[15]   R.W. Tejwani, M.E. Davis, B.D. Anderson, T.R. Stouch, J. Pharm. Sci. 100
       (2011) 2136.

[16]   D. Hofmann, L. Fritz, J. Ulbrich, C. Schepers, M. Böhning, Macromol. Theory
       Simul. 9 (2000) 293.

[17]   J.A. Lemkul, D.R. Bevan, J.Phys. Chem. B 114 (2010) 1652.

[18]   T.-X. Xiang, B.D. Anderson, J. Pharm. Sci. 93 (2004) 855.

[19]   D.B. Warren, D.K. Chalmers, C.W. Pouton, Mol. Pharm. 6 (2009) 604.

[20]   Y. Gao, K.W. Olsen, Mol. Pharm. 10 (2013) 905.

[21]   T. Xiang, B.D. Anderson, J. Pharm. Sci. 102 (2013) 876.

[22]   T.-X. Xiang, B.D. Anderson, J. Pharm. Sci. (2014) n/a.

[23]   P. Feenstra, M. Brunsteiner, J. Khinast, Int. J. Pharm. 431 (2012) 26.

[24]   W.L. Jorgensen, Acc. Chem. Res. 22 (1989) 184.

[25]   J.P. Valleau, D.N. Card, J. Chem. Phys. 57 (1972) 5457.

[26]   G.M. Torrie, J.P. Valleau, J. Comput. Phys. 23 (1977) 187.

[27]   J. Aquist, C. Medina, J.E. Samuelson, Protein Eng. 7 (1994) 385.

[28]   T. Hansson, J. Marelius, J. Aquist, J. Comput. Aid. Mol. Des. 12 (1998) 27.

[29]   I.D. Wall, a R. Leach, D.W. Salt, M.G. Ford, J.W. Essex, J. Med. Chem. 42
       (1999) 5142.

[30]   M.K. Gilson, H.-X. Zhou, Annu. Rev. Biophys. Biomol. Struct. 36 (2007) 21.

[31]   Y. Su, E. Gallicchio, K. Das, E. Arnold, R.M. Levy, J. Chem. Theory Comput. 3 (2007) 256.

[32]   D.A. Pearlman, D.A. Case, J.W. Caldwell, W.S. Ross, T.E. Cheatham III, S. DeBolt, D. Ferguson, G. Seibel, P. Kollman, Comp. Phys. Commun. 91 (1995) 1.

[33]   D.A. Case, T.E. Cheatham III, T.A. Darden, H. Gohlke, R. Luo, K.M. Merz, C. Onufriev, C.L. Simmerling, B. Wang, R. Woods, J. Comput. Chem. 26 (2005) 1668.

[34]   D.A. Case, T.A. Darden, T.E. Cheatham, C.L. Simmerling, J. Wang, R.E. Duke, R. Luo, R.C. Walker, W. Zhang, K.M. Merz, B. Roberts, B. Wang, S. Hayik, A. Roitberg, G. Seabra, I. Kolossváry, K.F. Wong, F. Paesani, J. Vanicek, X. Wu, S.R. Brozell, T. Steinbrecher, H. Gohlke, Q. Cai, X. Ye, M.-J. Hsieh, G. Cui, D.R. Roe, D.H. Mathews, M.G. Seetin, C. Sagui, V. Babin, T. Luchko, S. Gusarov, A. Kovalenko, P.A. Kollman, Univ. California, San Fr. 11 (2010).

[35]   W.L. Jorgensen, J. Tirado-Rives, J. Am. Chem. Soc. 110 (1988) 1657.

[36]   J.C. Berendsen, D. van der Spoel, R. van Drunen, Comp. Phys. Com. 91 (1995) 43.

[37]   E. Lindahl, B. Hess, D. van der Spoel, J. Mol. Mod. 7 (2001) 306.

[38]   D. van der Spoel, E. Lindahl, B. Hess, G. Groenhof, A.E. Mark, J.C. Berendsen, J. Comp. Chem. 26 (2005) 1701.

[39]   B. Hess, C. Kutzner, D. van der Spoel, E. Lindahl, J. Chem. Theory Comput. 4 (2008) 435.

[40]   W. Humphrey, A. Dalke, K. Schulten, J. Molec. Graph. 14 (1996) 33.

[41]   U. Essmann, L. Perela, M.L. Berkowitz, T. Darden, H. Lee, L.G. Pedersen, J. Chem. Phys 103 (1995) 8577.

[42]   A.M. Evans, B.L. Holian, J. Chem. Phys. 85 (1983) 4069.

[43]   J.C. Berendsen, J.P.M. Postma, W.F. van Gunsteren, A. DiNola, J.R. Haak, J. Chem. Phys. 81 (1984) 3684.

[44]   J.E. Mark, Polymer Data Handbook, Oxford University Press, Oxford, 1999.

[45]   W.F. van Gunsteren, J.C. Berendsen, Mol. Simul. 1 (1988) 173.

[46]   M.R. Shirts, J.D. Chodera, J. Chem. Phys. 129 (2008) 124105.

[47]   L.R. Snyder, J. Chromatogr. 92 (1974) 223.

[48]   B. Hess, N.F.A. Van Der Vegt, Macromolecules (2008) 7281.

Retention-time Prediction for Polycyclic Aromatic Compounds in Reversed-phase Electro-chromatography [6]

Log P_{O/w} based models are often used for the retention time prediction of reversed phase liquid chromatography. Here, we present the investigation of the applicability of log P_{O/w} based retention time predictions for the separation in capillary electro-chromatography (CEC). A test set of 5 polycyclic aromatic hydrocarbons was separated using two different stationary phases with three different mobile phases each. The resulting retention times were correlated with the experimental log P_{O/w} values as well as with calculated log P_{O/w} values. The used methods include quantitative structure property relationship (QSPR) models as well as molecular dynamic methods such as the linear interaction energy (LIE) or the Bennett acceptance ratio (BAR). The results indicate that rigorous simulation models are capable of accurately reproducing experimental results and that the electrophoretic mobility of analytes in CEC separations leads to significant deviations in the retention time prediction.

---

[6] This chapter is taken from a Journal article by Feenstra et al. submitted to the Journal of Molecular Modeling (2014)

Introduction

Liquid chromatography (LC) has evolved to become one of the most important techniques for the separation, isolation and purification of substances.[1] It is widely used in the chemical and pharmaceutical industry and its applications are widespread, ranging from small-scale analytical purposes with high sensitivity and resolution to large scale preparative purposes with a high throughput, e.g., for the purification of biotechnologically manufactured proteins.[2]

Among the various LC techniques reversed-phase (RP) chromatography has become the "working horse" mainly for analytical separation, due to its robustness and variability. The working principle of RP chromatography is that the components to be separated (analytes) are dissolved in a moving (mobile) phase and interact differently with a second non-moving (stationary) phase. The mobile phase is usually a polar (often aqueous) liquid and the stationary phase is a silica material, functionalized with alkyl chains.[3] The more or less distinct interactions between an analyte and the alkyl chains lead to a different pace at which an analyte travels through a stationary phase. This results in a characteristic retention time for any given analyte in a specific chromatographic system.

The separation effect is based on the molecular interactions between the analyte and either of the two phases. These interactions consist of a combination of van der Waals forces, Coulomb forces and hydrophobic interactions.[4] Macroscopically, these interactions can be expressed via the solvation free energy ($\Delta_{solv}G$) of the analyte in either one of the chromatographic phases. Since the measurement of the free energy is not a straightforward task, a very common way to express the interactions of an analyte in two different phases is to use the partition coefficient.[5] The partition coefficient is usually easy to obtain experimentally. A very commonly used partition coefficient in chemical and pharmaceutical sciences is the octanol-water partition coefficient $P_{o/w}$. This coefficient and its logarithmic form $\log P_{o/w}$ is used, for example, to characterize the distribution of an analyte into biological membranes. In RP chromatography it can be related to the retention time t_c in a chromatographic separation using Eq. (1).[6]

$$\log P_{o/w} = \log t_c + const \qquad (1)$$

with

$$t_c = \frac{(t_R - t_0)}{t_0} \qquad (2)$$

t_R is the retention time of the analyte and t_0 is the retention time of a completely unretained component (dead or residence time).

The prediction of the chromatographic retention becomes especially important in the case of the trace analysis of structural isomers. Since high-resolution mass-spectrometry-based detectors cannot differentiate between structural isomers a reliable method to predict the retention time would be highly beneficial for the identification of the analyte.[7] However, in some cases the experimental log $P_{o/w}$ value is not easily available. This is especially the case when there is no reference analyte at hand or it is too valuable to be used in flask experiments.

A very common method to estimate the log $P_{o/w}$ value is to use quantitative structure property relationship (QSPR) models. The idea behind QSPR models is to relate chemical structure elements of an analyte to its physicochemical properties, in this case the log $P_{o/w}$. QSPR models have the advantage to be very fast but require a large amount of empirical data to make sound predictions.[8] Furthermore, the accuracy and reliability of QSPR models is not always sufficient.

Alternatively, the calculation of the log $P_{o/w}$ can be performed using molecular simulations. Molecular simulations are based on atomistic properties and can be used to obtain detailed mechanistic insights. A feasible approach would be to calculate the solvation free energy $\Delta_{solv}G$ of the analytes in the two different solvents. The aforementioned relation between the free energy of solvation then yields the $P_{o/w}$ (Eq.(3)).

$$P_{o/w} = \exp\left(\frac{\Delta_{hyd}G - \Delta_{oct}G}{RT}\right) \qquad (3)$$

In Eq.(3) $\Delta_{hyd}G$ is the solvation free energy in water and $\Delta_{oct}G$ is the solvation free energy in octanol. R and T denote the gas constant and thermodynamic temperature, respectively.

In this work we correlate differently obtained $\log P_{o/w}$ values and other thermodynamic properties of 5 analytes with their retention times in capillary electro-chromatography (CEC). CEC deviates from conventional liquid chromatography such that the flow of the mobile phase is induced via an electric potential rather than pressure.[9] The generated electric field also induces a migration of charged or polar analytes similar to electrophoresis altering the retention time for those analytes compared to conventional chromatography. Therefore, a prediction of retention times becomes more elaborate for electro-chromatographic applications. In order to keep electrophoretic migration low the model system chosen for the separation is a set of non-polar polycyclic aromatic hydrocarbons (PAHs). For each PAH the experimentally determined $\log P_{o/w}$ is taken from literature and compared to the predicted $\log P_{o/w}$ from a QSPR based model. Additionally, the octanol-water partition will also be estimated based on the linear interaction energy (LIE) algorithm [10] and free energy of solvation calculations using the Bennett acceptance ratio.[11]

Materials and Methods

Chemicals

Tetraethoxysilane (TEOS, 95% Fluka), triethoxy(octyl)silane (C$_8$-TEOS, 97.5%, Aldrich), hexadecetyltrimethylammonium bromide (CTAB, 98% Sigma), polygosil particles 60-5 (Lactan), diethylamine (99.5%, Fluka), (3-aminopropyl)triethoxysilane (APTES, >98%, Fluka), water (ultrapure, 0.06 µs/cm), ethanol (1% MEK, Roth), HCl (32% p.a., Roth), NaOH (99%, p.a.), MeOH (99%, Roth)

Analytes

The following polycyclic hydrocarbons (PAHs) were used as analytes for the separation experiments: Napthalene (98%, Fluka), acenaphthylene (75%, Aldrich), phenanthrene (98%, Aldrich), anthracene (96%, Fluka), pyrene (98%, Aldrich),

fluoranthene (98%, Aldrich). Thiourea (>99%, Sigma-Aldrich) was used as non-interacting tracer for the determination of the dead-time.

Mobile phase

Different kinds of mobile phases were used: (1) a 1:4 mixture of citrate buffer and methanol, (2) a 1:9 mixture of citrate buffer and methanol and (3) a 1:4 mixture of TRIS – buffer and acetonitrile (ACN). The alkaline TRIS buffer with 25 mmol/L tris(hydroxylmethyl)aminomethane (TRIS) was prepared in bi-distilled water. The acid citrate buffer solution was prepared by mixing citric acid monohydrate (25 mmol/L) with bi-distilled water. All solvents for the buffer preparation were obtained from VWR International (Darmstadt, Germany) and filtered with a syringe filter (0.2 µm pore size) and degassed by sonication before use.

Stationary phase

Commercial CEC capillary (System: "Agilent"): Agilent CEC Cap HypC8 3µm, 100µm, 25cm

Manually prepared monolithic CEC capillary (System "TUG"):

To prepare the monolithic materials the following compounds were used (given amounts refer to 1 mol equiv. of TEOS): TEOS (1 mol equiv.), C_8-TEOS (0.4 mol equiv.), HCl (0.5 M, 0.01 mol equiv.), H_2O (1.25 mol equiv.), MeOH (22.2 mol equiv.) and polygosil particles (stabilizer, 15 wt%). This precursor mixture was stirred at 60°C for 3 h, cooled down to room temperature, and then, diethylamine (0.25 mol equiv.) was added. The liquid was then filled into the pretreated capillary by applying 1 bar with the help of a Merck Hitachi L-6200 HPLC-Pump. 25 cm of the capillary were filled with precursor mixture and 10 cm were left empty for creating a detection window afterwards. After the precursor mixture was filled into the capillary, it was sealed and left for polymerization overnight at 40°C. The filled capillaries were tested for their pressure resistance at 50 bar (using a Merck Hitachi L-6200 HPLC-Pump, flushing liquid: MeOH).[12]

CEC device

Agilent G1600A with a real-time UV-Visible diode array detector (190-600 nm).

Experimental log $P_{o/w}$ values

The experimental log $P_{o/w}$ values for each PAH were determined as the average value of all entries found in the reaxys database.[13] Table shows the average values composed from all literature sources including the standard deviation.[14–26]

QSPR based log $P_{o/w}$ values

The log $P_{o/w}$ values for the PAHs were calculated using the free ACD/LogP software (fragment based algorithm).[27]

Simulations

For our simulations all components were manually sketched using the AMBER11 [28–30] module xleap. The solvents used were water and octanol. The corresponding OPLS-AA (Optimized Potentials for Liquid Simulations – All Atoms) force-field [31] parameters (including charge) were applied to all atoms and simple point charge (SPC) water was used.[32] All MD simulations were performed using the GROMACS software package version 4.5.3.[33–36]

For the calculation of the free energy of solvation, the enthalpy and the Lennard-Jones contributions to the enthalpy, the API was placed inside a cubic box with the side length of 3 nm followed by solvation with the appropriate solvent at ambient density. Periodic boundary conditions were applied and all distance-dependent properties were cut off at 1 nm. Long-range electrostatics was accounted for using particle mesh Ewald.[37] The box was equilibrated at the temperature of 300 K. The pressure was held constant at 1 bar by a Parrinello-Rahman barostat [38] with a time constant of 0.5 ps and compressibility of 4.5×10^{-6} bar^{-1}. 5,000 steps of steepest descent minimization were followed by 5,000 steps of L-BFGS minimization, 50,000 steps of constant volume (NVT ensemble) and 50,000 steps of constant pressure (NPT ensemble) equilibration. The equations of motion were solved using an sd integrator [39] with a time step of 2 fs. Production runs for the calculations of free energies of solvation were performed at the following λ-values: {0.00, 0.05, 0.10, 0.15, 0.20, 0.25, 0.30, 0.35, 0.40, 0.45, 0.50, 0.55, 0.60, 0.65, 0.70, 0.75, 0.80, 0.85, 0.90, 0.95, 1.00}. Here, λ denotes the coupling parameter describing interactions between the solute and the solvent. At λ = 0 all interactions (electrostatic and short-

range van der Waals interactions) were switched on and at the value of $\lambda = 1$ all interactions were switched off. Each run included 2,500,000 steps equaling 5 ns of simulation time. The ΔG_{solv} values were calculated using the GROMACS utility g_bar.[11,40] Enthalpy and Lennard-Jones contributions to the enthalpy were taken from the production run at $\lambda = 1$ using the gromacs utility g_energy.

For the calculation of the linear interaction energy (LIE) 3 analyte molecules were placed inside a cubic box with the side length of 4 nm followed by solvation with the appropriate solvent at ambient density. Periodic boundary conditions were applied and van der Waals interactions were cut off at 1.4 nm. Long-range electrostatics were accounted for using particle mesh Ewald [37]. The box was equilibrated at the temperature of 300 K using a Nosé-Hoover thermostat.[41] The pressure was held constant at 1 bar by a Berendsen barostat with a time constant of 0.5 ps and compressibility of 4.5×10^{-5} bar^{-1}.[42] 5,000 steps of steepest descent minimization were followed by 100,000 steps of equilibration. The equations of motion were solved using an md integrator with a time step of 2 fs. Production runs for the LIE calculations spanning 1 ns of simulation time were performed for each migrant molecule – solvent pair. Commonly, the LIE algorithm is used for the estimation of relative protein-ligand binding affinities.[43,44] Its advantage lies in its lower computational demand compared to other computational methods, such as thermodynamic integration or Bennett acceptance ratio, because it requires only two MD simulations for each investigated system: one with the analyte in solution (free state) and the other with the analyte "bound" to the stationary phase. The electrostatic and van der Waals interactions in the free and in the bound state are computed and the binding free energy can be estimated by a linear combination of these values.[45,46] The LIE does not directly take entropic contributions to the free energy into account.

Interaction energies between the analyte and the solvent were analyzed using the GROMACS utility *g_lie* with default parameters. VMD 1.8.7 [47] was used to visually analyze the investigated systems.

Results and Discussion

The retention times of 5 different PAHs were measured using CEC. The separation was performed using a combination of 3 different mobile phases and 2 different stationary phases. The mobile phases used were two different methanol-water mixtures and one acetonitrile-water mixture, while the stationary phases were a commercially available C8-capillary by Agilent and a manually prepared monolithic C8-capillary (TUG). Table 1 lists the logarithm of the experimentally determined net retention time (log t_c) for each individual analyte in the different chromatographic systems.

Table 1. Experimentally determined log t_c values of the different analytes for the different combinations of mobile and stationary phases

Mob. Phase:	H_2O:MeOH 1:4		H_2O:MeOH 1:9		ACN	
Stat. Phase:	Agilent	TUG	Agilent	TUG	Agilent	TUG
Naphthalene	1.13	0.86	0.50	0.46	0.70	0.70
Acenaphthylene	1.19	0.97	0.58	0.54	0.80	0.78
Anthracene	1.39	1.19	0.77	0.72	1.03	0.89
Fluoranthene	1.48	1.35	0.91	0.85	1.16	1.00
Pyrene	1.53	1.42	0.99	0.92	1.23	1.07

Here, it can be mentioned that the best separation (expressed via the separation factor α, Eq.(4)) can be achieved using a combination of the TU Graz capillary with the H_2O:MeOH 1:4 mobile phase followed by the combination of the Agilent capillary with ACN.

$$\alpha = \frac{t_{c,2}}{t_{c,1}} \qquad (4)$$

The properties that were then correlated with the retention times are listed in Table . The log $P_{o/w}$ is the experimentally determined octanol/water partition coefficient while log $P_{o/w,calc}$ is a directly calculated octanol/water partition coefficient based on molecular fragment contributions. ΔG_{part} is the analytes' solvation free energy difference between octanol and water and is obtained from MD simulations. The free

energy difference obtained through the LIE algorithm (ΔG_{LIE}) is also obtained from MD simulations. The total enthalpy of the analyte in the two phases was also calculated via MD simulation. ΔH_{part} gives the enthalpy difference for the analytes between water and octanol. This way the entropic contribution can be elucidated to the free energy as the difference between ΔG_{part} and ΔH_{part}. The enthalpic contributions can be further divided into energy contributions stemming from Coulomb interactions or van der Waal interactions. The ΔH_{LJ} values represent only the analytes' van der Waals interaction differences in the two phases expressed via a Lennard-Jones potential neglecting all contributions stemming from charged groups. In the following all energy values are presented as their negative values to be directly proportional to log t_c.

Table 2. Analyte properties used to correlate with the retention times. All energies in [kJ/kmol]

	Naphthalene		Acenaphthylene		Anthracene		Fluoranthene		Pyrene	
log $P_{o/w}$	3.30	+/-0.07	3.90	+/-0.15	4.53	+/-0.09	5.08	+/-0.14	5.03	+/-0.14
log $P_{o/w,calc}$	3.45	+/-0.16	4.27	+/-0.28	4.68	+/-0.17	5.17	+/-0.17	4.82	+/-0.27
-ΔG_{part}	22.50	+/-0.23	27.78	+/-0.16	30.65	+/-0.28	36.62	+/-0.35	35.44	+/-0.38
-ΔG_{LIE}	4.32	+/-0.52	3.15	+/-0.52	5.14	+/-0.45	3.25	+/-0.63	3.07	+/-0.53
-ΔH_{part}	5.59	+/-1.03	12.18	+/-1.27	11.80	+/-1.14	17.98	+/-1.58	17.99	+/-1.33
-ΔH_{LJ}	24.99	+/-0.89	29.11	+/-1.00	35.57	+/-0.79	38.28	+/-1.51	40.58	+/-0.97

The properties listed in Table 2 were then correlated with the net retention times to yield the following correlations. In Figure 1 we see the correlation between the experimental log $P_{o/w}$ and the net retention time for the 6 chromatographic systems.
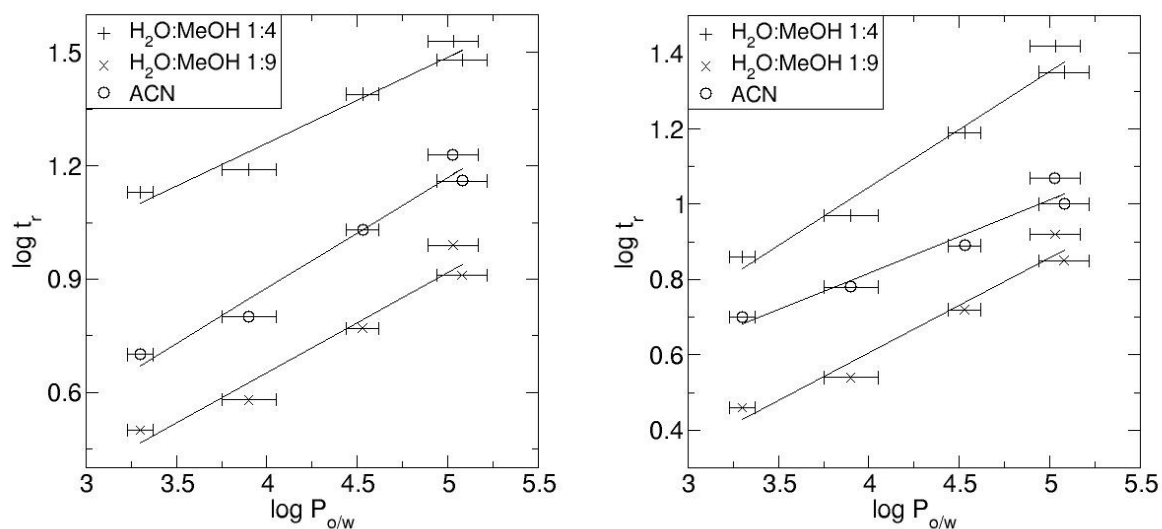
Figure 1. Correlation between log t_r and the experimental log $P_{o/w}$ for the system "Agilent" (left) and for the system "TU Graz" (right)

For all systems the correlation is acceptable with correlation coefficients R^2 ranging from 0.94 to 0.97 (Table 3) and minor deviations from the trend line resulting in an overestimation of the retention time for acenaphthylene and fluoranthene. Acenaphthylene and fluoranthene are, in contrast to the other analytes, not symmetrical in regard to their atomic charge distribution, and therefore, have non-zero values for their dipole moment. This is most likely the cause for lower than expected retention times stemming from the higher mobility in the electro-chromatographic system. In the case of fluoranthene this deviation leads to the prediction of an inversed retention order in regard to pyrene. When no structural identification is performed after the separation this issue will clearly lead to a misinterpretation of a separation experiment, and therefore, has to be regarded as a major issue.

When using a log $P_{o/w}$ calculated from molecular structures instead of using experimental values the retention order stays the same as for the experimental log $P_{o/w}$ values. However, the correlation quality as well as the precision of the single values decreases significantly as can be seen in Figure 2.
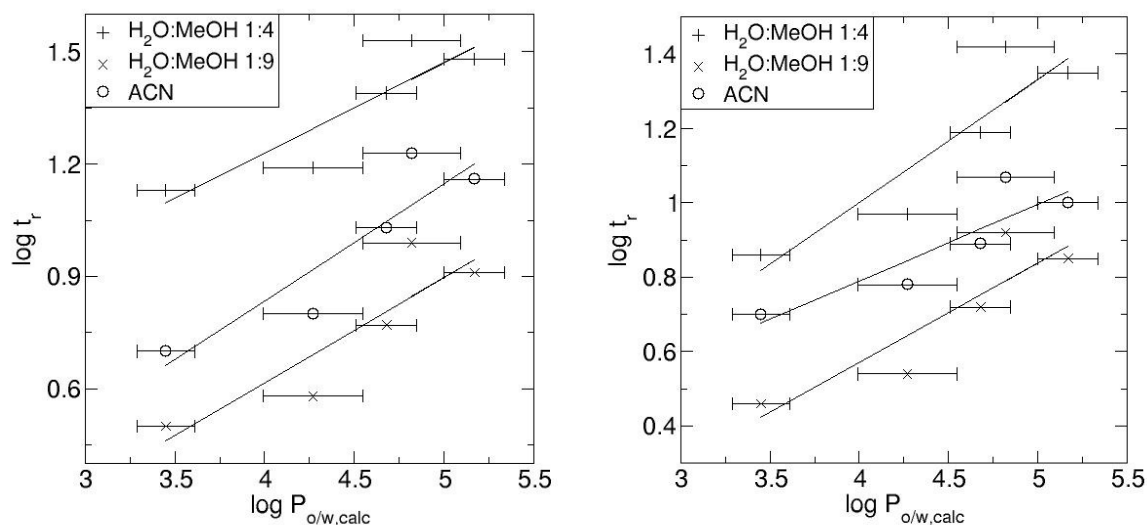
Figure 2. Correlation between $\log t_r$ and the calculated $\log P_{o/w}$ for the system "Agilent" (left) and for the system "TU Graz" (right)

The values are entailed with a higher uncertainty and a higher deviation from the trend and the problem of the incorrectly predicted retention order of fluoranthene and pyrene intensifies. This is also reflected by the correlation coefficients (R^2), in this case ranging from 0.79 to 0.82.

A more rigorous calculation of the $\log P_{o/w}$ via MD simulations yields ΔG_{part} values that are almost completely equivalent to the experimental $\log P_{o/w}$ values. Therefore, an estimation of the retention time using the ΔG_{part} values yields very similar results as the experimental $\log P_{o/w}$ values with R^2 ranging between 0.91 and 0.94 (Figure 3).
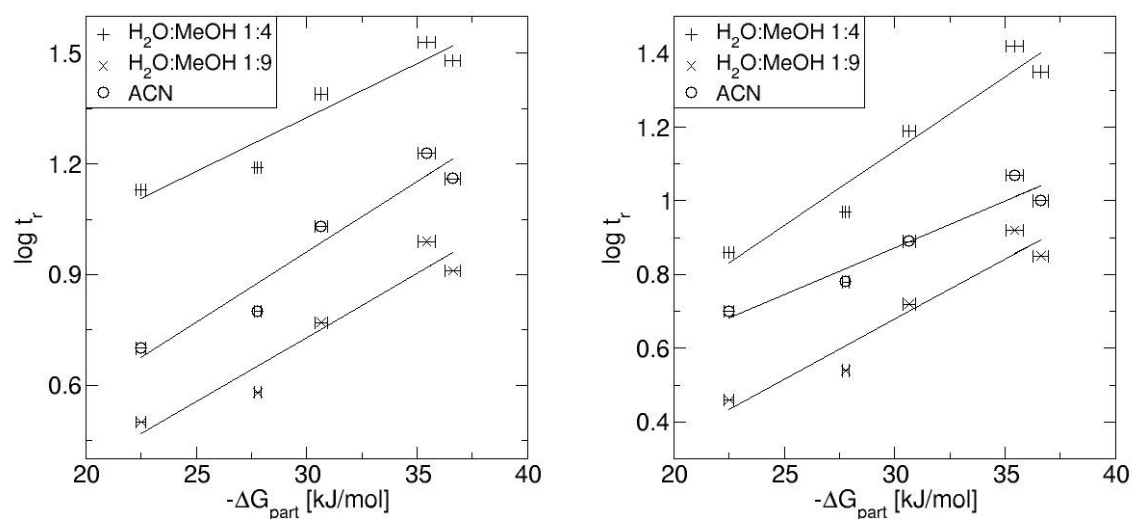
Figure 3. Correlation between $\log t_r$ and the analytes' free energy of solvation difference between octanol and water for the system "Agilent" (left) and for the system "TU Graz" (right)

Again, the retention time is overestimated for acenaphthylene and fluoranthene. However, the simulated $\log P_{o/w}$ can reproduce the experimental $\log P_{o/w}$ ($R^2= 0.99$) with high accuracy. This means that the energy of the analytes in both phases is calculated correctly. This renders it possible to further amplify the prediction capability of such MD simulations via the implementation of more detailed stationary phases. One could, for example, consider chemical modifications other than carbon chains or a detailed pore structure and the (reduced) transport of the analytes through such structures. However, the accuracy of prediction for this system is already high and deviations most likely stem from higher mobility of the analytes with dipole moment. Therefore, in a rigorous prediction model this phenomenon should be tackled first.

When the partition free energy is calculated using the LIE algorithm, the estimation of the retention time completely fails. No correlation or trend can be established (R^2 ranging from 0.06 to 0.15). Generally, the LIE is used for the estimation of binding energies between ligands and receptors. The LIE method works with significant simplifications compared to the Bennett acceptance ratio, especially when it comes to entropic contributions to the free energy. A further clarification of this matter can

be gained by the examination of the total enthalpy of the system. Figure 4 correlates the enthalpy difference (ΔH_{part}) between octanol and water.
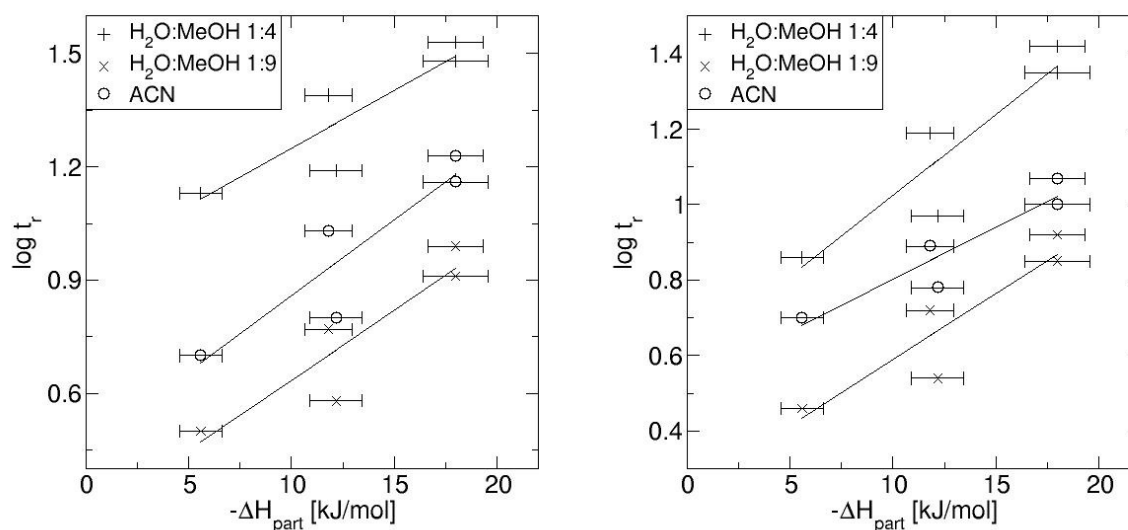

Figure 4. Correlation between log t_r and the analytes' enthalpy difference between octanol and water for the system "Agilent" (left) and for the system "TU Graz" (right)

Compared to the methods above it can be seen that the general trend is predicted with a moderate accuracy (R^2 from 0.80–0.87) with the common problem of insufficient resolution of fluoranthene and pyrene. Additionally, the retention time of acenaphthylene is strongly overestimated to an extent where the prediction of the retention order is wrong. Considering the complete lack of entropic contributions to this correlation it is surprisingly accurate compared to the LIE method. Since the LIE strongly depends on the Coulombic contributions to the free energy we stripped the enthalpy of the Coulombic contributions leaving only the van der Waals contributions and again correlated these values with the retention times.

Figure 5 shows the analytes' van der Waals interaction energy difference between octanol and water.
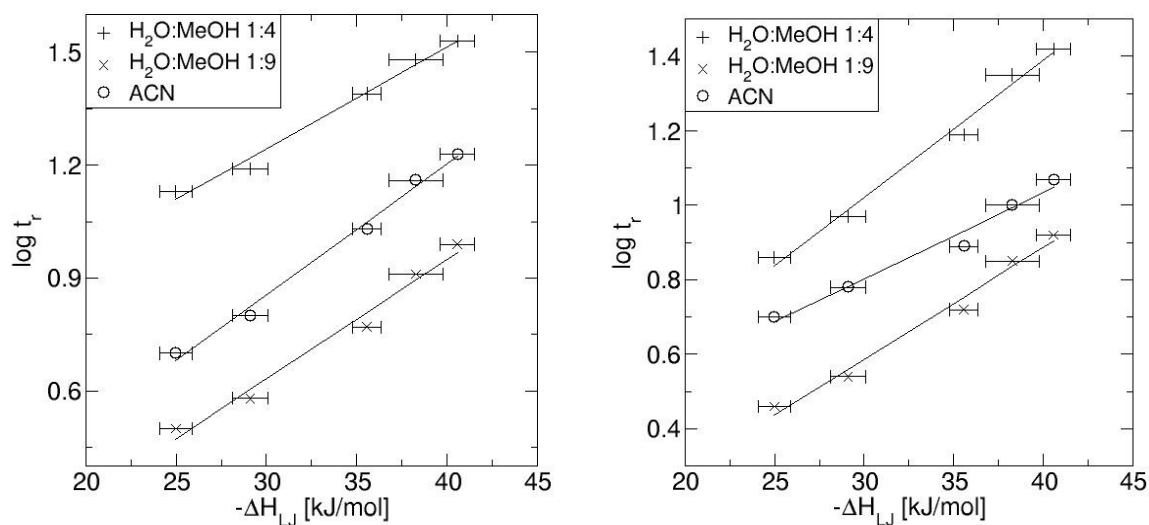
Figure 5. Correlation between log t_r and the analytes' van der Waals interaction energy difference between octanol and water for the system "Agilent" (left) and for the system "TU Graz" (right)

In this case entropic contributions, as well as Coulombic contributions are neglected. Interestingly, the correlation with the net retention time is highly accurate with correlation coefficients of 0.98 and 0.99. Furthermore, the retention order of all analytes is predicted correctly, in contrast to all former attempts. The reasons for that are (1) the difference in entropy between octanol and water is similar for all analytes, and therefore, can be neglected for the given system (this can be verified using the data at hand) and (2) charges only play a minor role in the partition of the non-polar analytes, and thus, the Coulombic contributions can be neglected. Apparently, the inaccuracy from obliterating the Coulombic interactions during the partition prediction cancels the inaccuracy from not including the effect of the electric field on the analytes mobility. In summary it is observed, that this highly reduced model is better suited to approximate the electro-chromatographic separation of PAHs than experimental log $P_{o/w}$ values. Of course it has to be stated that the introduction of polar analytes would obliterate any attempt to predict retention times without considering the Coulombic interactions.

Table 3. Correlation coefficients (R^2) for the different systems

Mob. Phase:	H$_2$O:MeOH 1:4		H$_2$O:MeOH 1:9		ACN		Average
Stat. Phase:	Agilent	TUG	Agilent	TUG	Agilent	TUG	
log P$_{o/w}$	0.96	0.97	0.95	0.96	0.96	0.94	**0.96**
log P$_{o/w,calc}$	0.82	0.82	0.79	0.79	0.82	0.80	**0.81**
-ΔG_{part} [kJ/mol]	0.91	0.94	0.92	0.92	0.92	0.92	**0.92**
-ΔG_{LIE} [kJ/mol]	0.06	0.10	0.11	0.11	0.08	0.15	**0.10**
-ΔH_{part} [kJ/mol]	0.80	0.85	0.84	0.84	0.83	0.87	**0.84**
-ΔH_{LJ} [kJ/mol]	0.99	0.99	0.98	0.98	0.99	0.98	**0.98**

Summary and Outlook

The experimentally determined log P$_{o/w}$, a QSPR based log P$_{o/w}$, as well as the free energy difference in octanol and water were correlated with the chromatographic net retention times for a set of 5 PAHs. Additionally, the free energy difference using the LIE algorithm as well as the enthalpy difference and the difference in van der Waals interactions between octanol and water were correlated. A comparison of the obtained correlations yields the following results:

- The experimental log P$_{o/w}$ correlates well with the net retention times (avg. R^2= 0.96) of the analytes while for 2 analytes the prediction of the retention order was wrong.

- The QSPR based log P$_{o/w}$ is significantly inferior to the experimental log P$_{o/w}$ accuracy-wise (avg. R^2= 0.81) while qualitatively yielding the same results.

- The free energy difference between octanol and water calculated with the Bennett acceptance ratio can be used to accurately calculate the experimental log P$_{o/w}$. This means that the energy of the analytes in both phases is calculated correctly.

- The free energy difference between octanol and water calculated with the LIE does not correlate with the retention times of the PAHs.

- The analytes' enthalpy difference between octanol and water correlates moderately (avg. R^2= 0.84) while a correct retention order cannot be predicted due to large overlapping of confidence intervals for the individual analytes.

- The calculation of the analytes' van der Waals interactions differences in octanol and water yields the best correlation with their net retention times (avg. $R^2 = 0.98$). However, this is only possible for non-polar analytes due to the complete neglect of Coulomb interactions.
- Analytes with a non-zero dipole moment have a higher mobility in the investigated systems. This phenomenon is not covered using log $P_{o/w}$ based prediction models.

As a consequence of these findings our next step in the investigation of separation in electro-chromatography will be the analysis of polar molecules. For the accurate prediction of retention times of polar analytes the effect of their electrophoretic mobility has to be taken into account. Furthermore, based on the highly accurate calculation of the free energies in the investigated systems an extension of the simulations towards detailed stationary phases looks highly promising. The implementation of different functional groups as well as the pore structure of stationary phase material offers possibilities not covered by simple partition based prediction methods.

Acknowledgements

References

[1]   A. Braithwaite, F.J. Smith, Chromatographic Methods, Kluver Academic
        Publishers, Dordrecht, 1999.

[2]   R.Q. Thompson, J. Chem. Educ. 77 (2000) 453.

[3]   J.J. Pesek, M.T. Matyska, in:, J. Cazes (Ed.), Encycl. Chromatogr., Taylor and
        Francis Group, Boca Raton, 2005.

[4]   C.F. Poole, in:, C.F. Poole, M. Cooke (Eds.), Encycl. Sep. Sci., Academic
        Press, New York, 2000.

[5]   G. Eugene Kellogg, D.J. Abraham, Eur. J. Med. Chem. 35 (2000) 651.

[6]   M. Mirrlees, S. Moulton, C. Murphy, P. Taylor, J. Med. Chem. 19 (1976) 615.

[7]   E. Tyrkkö, A. Pelander, I. Ojanperä, Anal. Chim. Acta 720 (2012) 142.

[8]   R. Kaliszan, T. Bączek, in:, T. Puzyn, J. Leszczynski, M.T. Cronin (Eds.),
        Recent Adv. QSAR Stud. SE - 8, Springer Netherlands, 2010, pp. 223–259.

[9]   M.P. Henry, C.K. Ratnayake, in:, J. Cazes (Ed.), Encycl. Chromatogr., Taylor
        and Francis Group, Boca Raton, 2005.

[10]   J. Aquist, C. Medina, J.E. Samuelson, Protein Eng. 7 (1994) 385.

[11]   C.H. Bennett, Comp. Phys. 22 (1976) 245.

[12]   M. Braunbruck, Preparation, Characterization and Simulation of Functionalized
        Monolithic Materials for Electrochromatography, TU Graz, 2013.

[13]   (2014).

[14]   F.-D. Kopinke, J. Poerschmann, U. Stottmeister, Environ. Sci. Technol. 29
        (1995) 941.

[15]   P.G.-J. de Maagd, D.T.E.M. ten Hulscher, H. van den Heuvel, A. Opperhuizen,
        D.T.H.M. Sijm, Environ. Toxicol. Chem. 17 (1998) 251.

[16]   P. Ruelle, U.W. Kesselring, J. Pharm. Sci. 87 (1998) 987.

[17]   W. Chen, A.T. Kan, G. Fu, L.C. Vignona, M.B. Tomson, Environ. Toxicol. Chem. 18 (1999) 1610.

[18]   V. Pichon, TrAC Trends Anal. Chem. 18 (1999) 219.

[19]   K. Valko, C.M. Du, C. Bevan, D.P. Reynolds, M.H. Abraham, Curr. Med. Chem. 8 (2000) 1137.

[20]   R.S. Brown, P. Akhtar, J. Åkerman, L. Hampel, I.S. Kozin, L.A. Villerius, H.J.C. Klamer, Environ. Sci. Technol. 35 (2001) 4097.

[21]   G. Byrns, Water Res. 35 (2001) 2523.

[22]   L.L.. van Stee, P.E.. Leonards, W.M.G.. van Loon, A. Jan Hendriks, J.L. Maas, J. Struijs, U.A.T. Brinkman, Water Res. 36 (2002) 4455.

[23]   S. Jurjanz, G. Rychen, J. Agric. Food Chem. 55 (2007) 8800.

[24]   J. Poerschmann, U. Trommler, D. Fabbri, T. Górecki, Chemosphere 70 (2007) 196.

[25]   S. Viamajala, B.M. Peyton, L.A. Richards, J.N. Petersen, Chemosphere 66 (2007) 1094.

[26]   P.L. Ferguson, G.T. Chandler, R.C. Templeton, A. DeMarco, W.A. Scrivens, B.A. Englehart, Environ. Sci. Technol. 42 (2008) 3879.

[27]   (2013).

[28]   D.A. Pearlman, D.A. Case, J.W. Caldwell, W.S. Ross, T.E. Cheatham III, S. DeBolt, D. Ferguson, G. Seibel, P. Kollman, Comp. Phys. Commun. 91 (1995) 1.

[29]   D.A. Case, T.E. Cheatham III, T.A. Darden, H. Gohlke, R. Luo, K.M. Merz, C. Onufriev, C.L. Simmerling, B. Wang, R. Woods, J. Comput. Chem. 26 (2005) 1668.

[30]   D.A. Case, T.A. Darden, T.E. Cheatham, C.L. Simmerling, J. Wang, R.E.
       Duke, R. Luo, R.C. Walker, W. Zhang, K.M. Merz, B. Roberts, B. Wang, S.
       Hayik, A. Roitberg, G. Seabra, I. Kolossváry, K.F. Wong, F. Paesani, J.
       Vanicek, X. Wu, S.R. Brozell, T. Steinbrecher, H. Gohlke, Q. Cai, X. Ye, M.-J.
       Hsieh, G. Cui, D.R. Roe, D.H. Mathews, M.G. Seetin, C. Sagui, V. Babin, T.
       Luchko, S. Gusarov, A. Kovalenko, P.A. Kollman, Univ. California, San Fr. 11
       (2010).

[31]   W.L. Jorgensen, J. Tirado-Rives, J. Am. Chem. Soc. 110 (1988) 1657.

[32]   D. van der Spoel, P.J. van Maaren, J.C. Berendsen, J. Chem. Phys. 108
       (1998) 10220.

[33]   J.C. Berendsen, D. van der Spoel, R. van Drunen, Comp. Phys. Com. 91
       (1995) 43.

[34]   E. Lindahl, B. Hess, D. van der Spoel, J. Mol. Mod. 7 (2001) 306.

[35]   D. van der Spoel, E. Lindahl, B. Hess, G. Groenhof, A.E. Mark, J.C.
       Berendsen, J. Comp. Chem. 26 (2005) 1701.

[36]   B. Hess, C. Kutzner, D. van der Spoel, E. Lindahl, J. Chem. Theory Comput. 4
       (2008) 435.

[37]   U. Essmann, L. Perela, M.L. Berkowitz, T. Darden, H. Lee, L.G. Pedersen, J.
       Chem. Phys 103 (1995) 8577.

[38]   M. Parrinello, A. Rahman, J. Appl. Phys. 52 (1981) 7182.

[39]   W.F. van Gunsteren, J.C. Berendsen, Mol. Simul. 1 (1988) 173.

[40]   D. Wu, D.A. Kofke, J. Chem. Phys. 123 (2005) 84109.

[41]   A.M. Evans, B.L. Holian, J. Chem. Phys. 85 (1983) 4069.

[42]   J.C. Berendsen, J.P.M. Postma, W.F. van Gunsteren, A. DiNola, J.R. Haak, J.
       Chem. Phys. 81 (1984) 3684.

[43]   T. Hansson, J. Marelius, J. Aquist, J. Comput. Aid. Mol. Des. 12 (1998) 27.

[44] I.D. Wall, a R. Leach, D.W. Salt, M.G. Ford, J.W. Essex, J. Med. Chem. 42
      (1999) 5142.

[45] M.K. Gilson, H.-X. Zhou, Annu. Rev. Biophys. Biomol. Struct. 36 (2007) 21.

[46] Y. Su, E. Gallicchio, K. Das, E. Arnold, R.M. Levy, J. Chem. Theory Comput. 3
      (2007) 256.

[47] W. Humphrey, A. Dalke, K. Schulten, J. Molec. Graph. 14 (1996) 33.

Summary of Major Findings

The investigation of the influence of the liquid phase composition on the solute-solid interaction in chapter "Prediction of Drug-Packaging Interactions via Molecular Dynamics (MD) Simulations" yielded the following results:

- The investigated simulation method can be used to predict the octanol/water partition coefficient based on a calculation of the solvation free energy.

- The calculation of the free energy of adsorption using the linear interaction energy algorithm (LIE), did not yield significant differences for the binding free energy between the solute and the polymer's surface for all investigated organic solvents. For water the obtained value indicated no adsorption of the solute to the surface. This does not agree with the results obtained from direct calculations of potentials of mean force between the solute and the surface.

- A different approach – a direct calculation of the potential of mean force between a molecule in solution and a container wall – yielded results for the free energy of adsorption that correlate well with the polarity index of the used solvent, which agrees with published experimental results.

- The results furthermore indicate that, generally, MD methods and, specifically, the OPLS-AA parameters used in our studies can successfully be used to investigate such solid-liquid interactions for different pure solvents as well as for binary mixtures.

- Although only the adsorption of solute molecules on polymers was investigated in the simulations, the results correlate with the findings from leaching experiments (the migration into/out of the polymer by either the migrating component or the solvent would in principle be possible. However, due to the small timescales examined this cannot be observed). This indicates that the contributions relating to the migration into/out of the polymer do not depend on the used solvent. Further experiments to clarify this statement are necessary.

- Since many drug products have a rather complex composition, simple polarity-based models for the prediction of drug packaging interactions might be insufficient. A more rigorous modeling approach, that is capable of including additional parameters, e.g., cosolvents or ionic strength, such as the method described in this work, might help overcome such difficulties.

The chapter "Investigation of Migrant – Polymer Interaction in Pharmaceutical Packaging Material using the LIE Algorithm" that investigated the free energy differences between a polymer solid phase and a liquid phase for small molecules yielded the following results:

- The use of molecular dynamics (MD) simulations for the calculation of the linear interaction energy (LIE) between a migrant and a polymer and solvent is a suitable approach for the prediction of the polymer – solvent partitioning behavior of the migrant. This somewhat contradicts the findings of the previous chapter. A discussion of this issue can be found in the outlook.

- The detailed model of the polymer and the migrant molecule is capable of incorporating interactions that are not accounted for by an empirical model based on the octanol/water partitioning coefficient ($P_{o/w}$) of the migrant.

- The used computational model is able to predict the behavior of two migrants better than an empiric $P_{o/w}$ based model.

- Furthermore, the comparison of the results for two different polymers showed that the calculated LIE values correlated well with experimental partitioning data without the need for an additional fit of parameters for the individual polymers.

The chapter "Retention-time Prediction for Polycyclic Aromatic Compounds in Reversed-phase Capillary Electro-chromatography" yielded the following results:

- The experimental log $P_{o/w}$ correlates well with the net retention times (avg. R^2= 0.96) of the analytes while for 2 analytes the prediction of the retention order was wrong.

- The QSPR based log $P_{o/w}$ is significantly inferior to the experimental log $P_{o/w}$ accuracy-wise (avg. R^2= 0.81) while qualitatively yielding the same results.

- The free energy difference between octanol and water calculated with the Bennett acceptance ratio can be used to accurately calculate the experimental log $P_{o/w}$. This means that the energy of the analytes in both phases is calculated correctly.

- The free energy difference between octanol and water calculated with the LIE does not correlate with the retention times of the PAHs.

- The analytes' enthalpy difference between octanol and water correlates moderately (avg. R^2= 0.84) while a correct retention order cannot be predicted due to large overlapping of confidence intervals for the individual analytes.

- The calculation of the analytes' van der Waals interactions differences in octanol and water yields the best correlation with their net retention times (avg. R^2= 0.98). However, this can only be obtained for non-polar analytes due to the complete neglecting of Coulomb interactions.

- Analytes with a non-zero dipole moment have a higher mobility in the investigated systems. This phenomenon is not covered using log $P_{o/w}$ based prediction models.

Outlook

As scientific research answers some questions it often raises new ones. During the work on this thesis certain issues or ideas emerged that could not be included in this work. The next section gives an overview of open topics and some ideas on how to deal with them.

Investigation of the restrictions of the Linear Interaction Energy Algorithm (LIE)

In this thesis the Linear Interaction Energy algorithm (LIE) was used with varying results. While the LIE was successfully applied for the prediction of the partition of different molecules between PVC and methanol a prediction failed when the partitioning of one migrant between a solid phase and different liquid phases especially water was calculated. Apparently, the LIE performs well, when the entropic contributions to the free energy in the solid and liquid phase are low or of comparable magnitude. Further investigation of the performance of the LIE is necessary. Especially an assessment of its performance when entropic contributions to the free energy are high should clarify this topic.

Drug – Packaging Interactions

In an attempt to further clarify the influence of the polymer properties on the free energy of adsorption the addition of plasticizer to the polymer could be investigated. Figure 1 shows the results of a first attempt on this endeavour. It shows the PMF curves for the adsorption of norepinephrine in ethanol on two different types of PVC. One PVC sample was generated without plasticizer; the other one with an amount of 40w% of di-2-ethylhexyl phthalate (DEHP) as plasticizer.
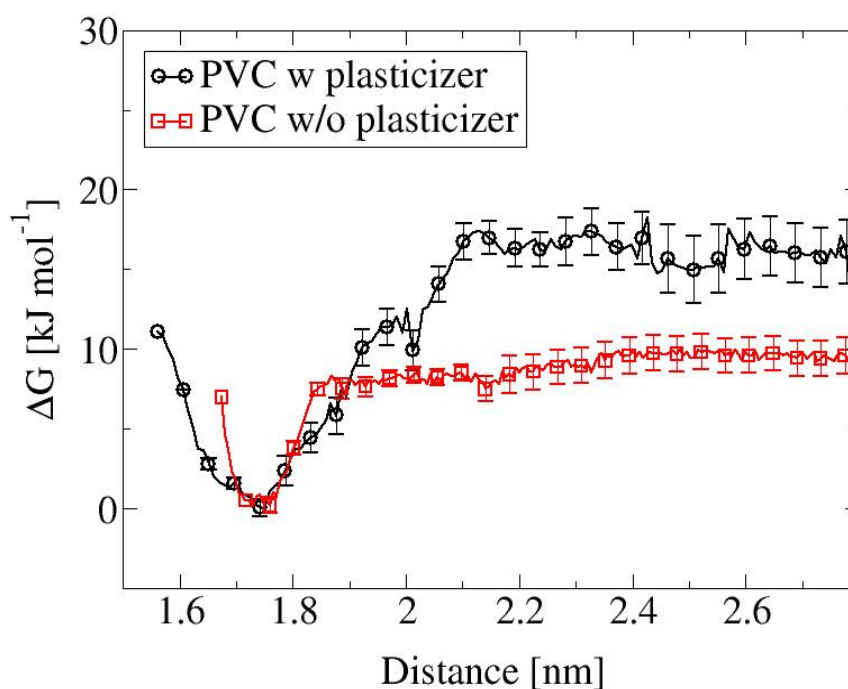
Figure 1 Potential of mean force curves for the adsorption of norepinephrine on two different PVC types in ethanol

There is a significant difference in the magnitude of the free energy of adsorption for the two different polymer samples. The plasticized PVC shows a larger difference in the values for the free energy of adsorption indicating that the adsorption is more likely to take place. Additionally, the potential well in the vicinity of the polymer surface is wider for the plasticized PVC while the slopes of the potential well are steeper for the non-plasticized PVC. This can be addressed to the higher mobility of the polymer chains in the plasticized PVC which results in a smoother repulsion of the migrating component by the polymer surface. Qualitatively, this result corresponds to empirical findings. A further study on this topic should clarify the quantitative influence of polymer additives on the solute uptake with the overall goal to find a model to predict and counteract dose fluctuations under real-life clinical conditions. After identification and understanding of the critical parameters responsible for drug- container-material interactions the gained knowledge could be used to create predictive tools for different drug-container systems. Ultimately, these predictive tools will result in a safer and more efficient administration of drugs to the patient in a clinical setting.

Chromatography

As a consequence of the findings in the chapter "Retention-time Prediction for Polycyclic Aromatic Compounds in Reversed-phase Capillary Electro-chromatography" the next step in the investigation of separation in electro-chromatography should be the analysis of polar molecules. For the accurate prediction of retention times of polar analytes the effect of their electrophoretic mobility has to be taken into account. Furthermore, based on the highly accurate calculation of the free energies in the investigated systems an extension of the simulations towards detailed stationary phases looks highly promising. The implementation of different functional groups as well as the pore structure of stationary phase material offers possibilities not covered by simple partition based prediction methods. To simulate the affinity and selectivity of the stationary phase for different solute molecules a representative part of the porous silica system could be modeled. This approach would include the modeling of a silica pore with functional groups attached to the surface. The solute molecules are then placed inside the pore that is filled with solvent molecules. Figure 2 schematically displays this approach.
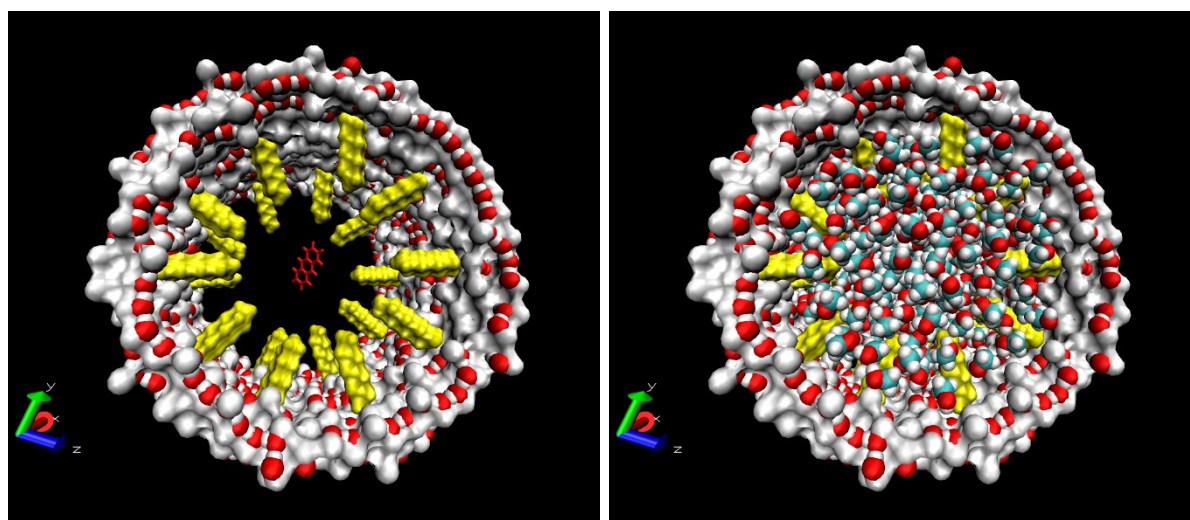

Figure 2 Pore with C_8-chains and anthracene molecule, empty (left) and filled with a mixture of methanol/water (right)

The measurement of the retention could be performed with a pull simulation where the solute is pulled through the pore and the force acting on the solute is registered. Alternatively, the trajectory of a solute moving freely through the pore could be analyzed and the diffusion coefficient calculated via the mean square displacement (MSD) over time. The idea behind this approach is that the flow of molecules is proportional to the diffusion coefficient and the retention time is proportional to the inverse of the flow. This way it should be possible to link the mobility of a solute molecule inside a pore to its retention behavior. In Figure 3 the approach is schematically displayed. It shows the mean square displacement of a solute molecule in a liquid (A). The black line represents the linear regression function of curve A. Its slope is proportional to the diffusion coefficient in the liquid. Curve B shows the mean square displacement of a solute molecule in the vicinity of a surface. The solute adsorbs on the surface after approx. 350 ps and detaches from the surface at approx. 650 ps. The red line also represents the linear regression for curve B but segmented into three parts. While the molecule is adsorbed on the surface its MSD stays constant since it is not able to move freely in the liquid. The dotted red line represents the overall linear regression of curve B resulting in a lower slope and therefore, in a lower diffusion coefficient.
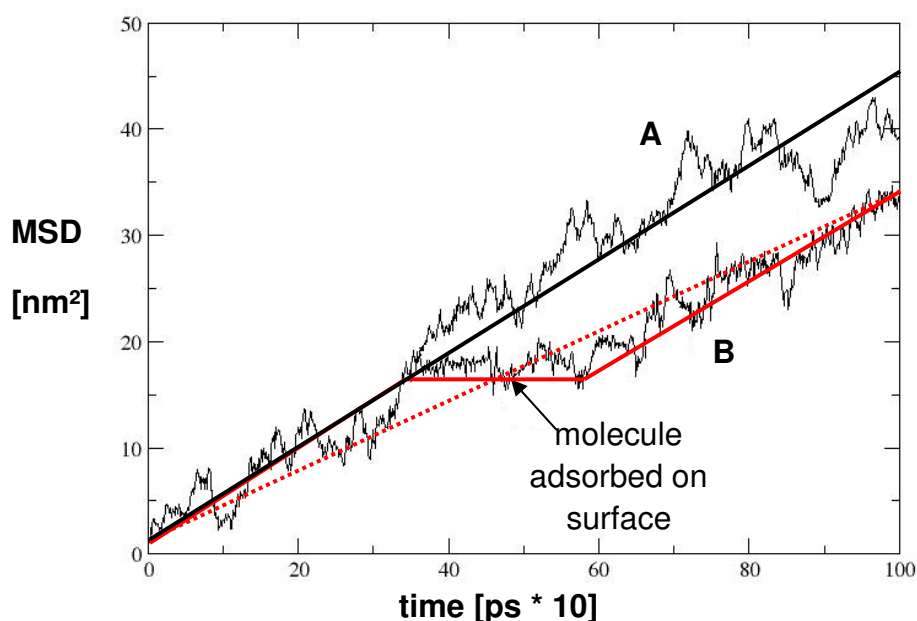

Figure 3 Mean square displacement of a solute molecule in a liquid (A) and in vicinity of a surface (B)

According to these considerations the relative decrease of the diffusion coefficient of a solute inside of the pore compared to the diffusion coefficient solely in the solvent corresponds to the relative amount of time the solute spends immobilized on the stationary phase via Eq. 1.

$$\frac{D_{pore}}{D_{solv}} = 1 - \frac{t_{stat}}{t_{tot}}$$

Eq. 1

D_{pore} diffusion coefficient inside the pore

D_{solv} diffusion coefficient in solvent

t_{stat} time the solute spends adsorbed to the stationary phase

t_{tot} total time

Use of Graphics Processing Units

During the work on this thesis powerful graphics processing units (GPUs) began to rise in popularity in the scientific community. GPUs, originally developed for rendering effects in computer games more and more become an alternative to common CPUs. A single GPU can nowadays easily outperform multi-processor core clusters and especially molecular simulations with their massive length and timescale restrictions could greatly benefit from this development.